UNIVERSITY OF CALIFORNIA, MERCED

MASTER'S THESIS

Exploration of Local Force Calculations Using the Methods of Regularized Stokeslets

by

Terese Thompson

A technical report submitted
in partial fulfillment of the requirements for the degree of

Master of Science in Applied Mathematics

2015

Committee Members:
Professor Karin Leiderman, Chair
Professor Arnold Kim
Professor François Blanchette

UNIVERSITY OF CALIFORNIA, MERCED
Graduate Division

This is to certify that I have examined a copy of a technical report by

Terese Thompson

and found it satisfactory in all respects, and that any and all revisions required by the examining committee have been made.

Applied Mathematics
Graduate Studies Chair:

_____
Professor Boaz Ilan

Thesis Committee:

_____
Professor Arnold Kim

Thesis Committee:

_____
Professor François Blanchette

Committee Chair / Research Advisor:

_____
Professor Karin Leiderman

_____
Date

Acknowledgements

Over more than the past two years, I have dedicated myself to further understanding Stokes' flow and in particular understanding and improving the Method of Regularized Stokeslets. This was my first time conducting mathematical research and, at first, the process seemed daunting. Thankfully, I had people to help me through as I learned how to cultivate my ideas and the ideas of others, and to stay organized and focused.

There were many people involved in this process. I would like to thank my advisor Prof. Karin Leiderman for suggesting the original research problem and staying involved in its evolution. She helped me in big ways and small ways like pushing me to be more organized and providing MATLAB on my computer. She was always there to listen to my ideas and offer some of her own. She helped me and this project stay focused. Without her, this thesis would not have come to fruition. I also appreciate the expertise and ideas from Postdoctoral Researcher Hoang-Ngan Nguyen in interpreting the results. While my advisor was away, she encouraged me to consult with Prof. François Blanchette who volunteered to help. He was also instrumental in this project. He offered his insight while my advisor was away and stayed involved after her return. He offered a different perspective and much helpful constructive criticism. I would also like to thank Prof. Arnold Kim for being on my committe and asking the questions that needed to be asked. My husband Peter helped me stay motivated on rough days, and his contribution of chocolate cannot be easily dismissed. I also owe my gratitued to my officemates Elizabeth Owens and Jason Davis who were always available when I needed someone to talk to about my research. Their steadfast support boosted my morale and helped keep me on task.

Contents

Exploration Localized Force Calculations Using the Methods of Regularized Stokeslets

by

Terese Thompson

Master of Science in Applied Mathematics

Professor Karin Leiderman, Chair

University of California, Merced

2015

Abstract

We analyze the performance of the Method of Regularized Stokeslets (MRS) and the Method of Auxiliary Regularized Stokeslets (MARS) in computing the forces necessary to translate a sphere with unit velocity in Stokes flow. In particular, we explore the dependence of local and global force calculations on various parameters associated with each method. The parameters we varied include the regularization parameter, the discretization of the sphere, and the spread and placement of the auxiliary Stokeslets (MARS only). One challenge when using the MRS is that there is no systematic way to choose the regularization parameter, and the error is sensitive to this choice. In the literature it is stated that, compared to the MRS, the MARS weakens the error dependence on the choice of regularization parameter. We found this to be true in some cases, but not in others. Specifically, the dependence is weakened when comparing the 1-norm of the global force error and 2-norm of the local force error. This behavior is not seen with the max-norm of the local force error. In addition, with the MARS, there is a strong dependence of error on the normalized patch length which controls the spread of the auxiliary Stokeslets. We find the conditions needed to optimize the MARS method to outperform the MRS on the translating sphere problem.

List of Symbols

- μ : viscosity
- $\mathbf{u}$: velocity
- p : pressure
- δ : Dirac delta function
- f : force
- $\mathbf{U}$: velocity of the sphere
- a : radius of the sphere
- N : number of (primary) Stokeslets
- ϵ : parameter that controls blob width
- ϕ_ϵ : regularized delta function
- E : normalized ϵ
- $normPL$: normalized Patch Length (of auxiliary Stokeslets)
- S : the Stokeslet matrix

List of Figures

1 Introduction

Creeping fluid flow or Stokes flow describes fluid flow where the viscous forces are high compared to the inertial forces. The study of Stokes' equations has been successfully employed to model a large number of real world phenomena such as the beating of cilia [1], sperm motility [2], and the interaction of swimming bacteria [3] to name a few.

The non-dimensional Stokes' equations for incompressible fluid flow are:

$$\mu\nabla^2\mathbf{u} = \nabla p - \mathbf{g} \tag{1}$$

$$\nabla \cdot \mathbf{u} = 0 \tag{2}$$

where $\mathbf{u}(\mathbf{x})$ is the velocity of the fluid, $p(\mathbf{x})$ is the pressure, μ is the dynamic viscosity, and $\mathbf{g}$ is the force per unit volume. These equations are linear, and by setting $\mathbf{g} = \mathbf{f}\delta(\mathbf{x} - \mathbf{x}_0)$ in equation 1 where δ is the Dirac delta function, we represent a singular point force of strength $\mathbf{f}$ at location $\mathbf{x}_0$. Using this point force, we find the fundamental solution, called the Stokeslet. In 3 dimensions the Green's solution of equations 1 and 2 is

$$\mathbf{u}_s(\mathbf{x}) = \frac{1}{8\pi\mu}\left(\frac{\mathbf{I}_3}{r} + \frac{(\mathbf{x}-\mathbf{x}_0)(\mathbf{x}-\mathbf{x}_0)}{r^3}\right)\mathbf{f} = \frac{1}{8\pi\mu}S(\mathbf{x},\mathbf{x_0})\mathbf{f}, \tag{3}$$

where $S(\mathbf{x},\mathbf{x_0})$ is the (singular) Stokeslet.

Oftentimes difficulty arises in the use of the Stokeslet when we are considering curves or points of force in $\mathbb{R}^3$ because the resulting integral formulation for the velocity is singular. In 2001, Ricardo Cortez published a numerical method called the Method of Regularized Stokeslets (MRS) [4]. The MRS sidesteps this difficulty by replacing the Dirac delta function in the formulation of the Green's solution with a regularized, radially symmetric δ function, ϕ_ϵ controlled by the parameter ϵ that controls the spread of the regularized delta function. (As ϵ goes to zero, we recover the singular Stokeslet.) By defining

$$\nabla^2 G_\epsilon(\mathbf{x}) = \phi_\epsilon(\mathbf{x})$$

and

$$\nabla^2 B_\epsilon(\mathbf{x}) = G_\epsilon(\mathbf{x})$$

we can state the solution for velocity of the resulting regularized system when we have N forces, $\mathbf{f}_k$, centered at $\mathbf{x}_k$ as

$$\mathbf{u}(\mathbf{x}) = \frac{1}{\mu}\sum_{k=1}^{N}\{(\mathbf{f}_k\cdot\nabla)\nabla B_\epsilon(\mathbf{x}-\mathbf{x}_k) - \mathbf{f}_k G_\epsilon(\mathbf{x}-\mathbf{x}_0)\} = \frac{1}{8\pi\mu}\sum_{n=1}^{N} S_\epsilon(\mathbf{x},\mathbf{x_0})\mathbf{f} \tag{4}$$

where G_ϵ and B_ϵ can be computed from the specific choice of ϕ_ϵ and $S_\epsilon(\mathbf{x},\mathbf{x_0})$ is the resulting regularized Stokeslet. Equation 4 can be used to impose velocity conditions on the discretized surface (or curve or collection of points) where the regularized point forces

are located

$$\mathbf{u}(\mathbf{x}_k) = \frac{1}{8\pi\mu}\sum_{n=1}^{N} S_\epsilon(\mathbf{x}_k, \mathbf{x}_n)\mathbf{f}_n, \tag{5}$$

where $\mathbf{x}_k$ are the locations of the Stokeslets. This equation can be interpreted in matrix form as

$$U = \frac{1}{8\pi\mu}SF. \tag{6}$$

The MRS has gained popularity as a numerical method, possibly due to the computational efficiency involved in having only a Lagrangian mesh of points with no underlying Eulerian grid for the fluid.

The MRS has two sources of error: the regularization and discretization errors. The regularization error is the result of replacing the Dirac delta function with the regularized approximation ϕ_ϵ in the calculation of the regularized Green's function. The discretization error comes from approximating the integral form of Green's solution:

$$\mathbf{u}(\mathbf{x}) \approx \frac{1}{8\pi\mu}\int_\partial S_\epsilon(\mathbf{x}, \mathbf{x}_0)\mathbf{f}ds(\mathbf{x}),$$

with a quadrature rule, usually the simple Riemann sum:

$$\mathbf{u}(\mathbf{x}) \approx \frac{1}{8\pi\mu}\sum_{n=1}^{N} S_\epsilon(\mathbf{x}, \mathbf{x}_n)\mathbf{f}_n.$$

The MRS shows great sensitivity to the choice of the parameter ϵ. That is to say that both the regularization and discretization error associated with the MRS varies significantly as ϵ is varied.

A systematic way of choosing ϵ to minimize error does not exist which motivated Barrero-Gil to develop an alternative method [5] the Method of Auxiliary Regularized Stokeslets (or MARS). Based on the MRS, the MARS introduces auxiliary Stokeslets into the system. The Stokeslets of the MRS are called primary Stokeslets, and each primary Stokeslet has associated with it a collection of nearby auxiliary Stokeslets that more finely discretize the surface or the curve; they lay on the surface or curve. When the effect of any primary Stokeslet on itself is calculated (the diagonal sub-matrices of S in equation 6), one averages the effects of the auxiliary Stokeslets on the location of the primary Stokeslet; this is the only use of auxiliary Stokeslets in the calculation. Consider $\mathbf{x}_k$ is the location of the kth primary Stokeslet, we then compute its velocity as

$$\mathbf{u}(\mathbf{x}_k) = \frac{1}{8\pi\mu}\langle S_\epsilon(\mathbf{x}_k, \mathbf{x}_a)\rangle\mathbf{f}_k + \frac{1}{8\pi\mu}\sum_{n=1, n\neq k}^{N} S_\epsilon(\mathbf{x}_k, \mathbf{x}_n)\mathbf{f}_n, \tag{7}$$

where $\mathbf{x_a}$ represents the locations of the auxiliary Stokeslets. The MARS succeeds in weakening the dependency of the regularization error on the parameter ϵ compared to the MRS. Barrero-Gil argues that this allows fewer primary Stokeslets to be used to ensure

accuracy [5]. This is important because fewer Stokeslets mean that the matrix S in equation 6 is smaller, and therefore, the equation is faster to solve. (When we evaluate the MARS in chapter 3, we make use of this fact.) However, many unanswered questions remain such as the ideal placement of the auxiliary Stokeslets.

Both Barrero-Gil and Cortez consider **global** measures of error in their examination of their respective methods. One such global measure of error is the traction error. For a sphere translating in Stokes' flow, the traction, $\mathbf{F}_T$ can be computed as the opposite of the total drag, $\mathbf{F}_D$ [6]:

$$\mathbf{F}_T = -\mathbf{F}_D = -\int_{\partial D} \boldsymbol{\sigma} \cdot \mathbf{n} dS = 6\pi\mu a \mathbf{U}, \tag{8}$$

where ∂D is the surface of the sphere, $\boldsymbol{\sigma}$ is the stress tensor, $\mathbf{n}$ is the unit normal vector to the surface of the sphere, μ is the viscosity of the fluid, a is the radius of the sphere, and $\mathbf{U}$ is the velocity of the sphere. When velocity is prescribed as $U_0\mathbf{e}_i$ on the sphere, equation 5 is used to compute the resulting calculated traction (after a solve of the matrix equation) as:

$$F_{T,calc} = \sum_{n=1}^{N} f_{i,n}. \tag{9}$$

Then, the relative traction error on the sphere is

$$Err_T = \frac{|F_{T,calc} - 6\pi\mu a U_0|}{|6\pi\mu a U_0|}. \tag{10}$$

The traction error tells us about close the **total** calculated force is to the analytic value. However, this measure of global error does not tell us how close each individual force, $\mathbf{f}_n$, is to its theoretical value. Traction error may give a sufficient evaluation of performance when a rigid body is immersed in Stokes' flow.

It is also important to consider the error of each $\mathbf{f}_n$, which we call the textbflocal error. In this paper, we consider $\mathbf{f}_A$ or force per area as the measure of local performance. This force is computed as

$$\mathbf{f}_{n,A} = \frac{\mathbf{f}_n}{P_{n,A}}, \tag{11}$$

where $P_{n,A}$ is the amount of surface area associated with the nth Stokeslet. In many places, the n subscripts are neglected when talking about f_A. We consider two measures of error associated with $\mathbf{f}_A$: a 2-norm error and a maximum error. We detail the calculation of these in section 2.3.

We examine the performance of the MRS and the MARS on the test problem of a sphere translating in free-space Stokes' flow. We prescribe the velocity and consider measures of the global and local error associated with the calculated force. Our primary concern is how the discretization of the sphere and parameters in each method affect the global and local error of the force calculation. We are especially interested in whether the local error is small for each $\mathbf{f}_n$ when the global error is small. In the MRS we consider the blob parameter: ϵ or ϵ normalized by Stokeslet spacing, E, as the parameter of interest. In the MARS, we consider E as well as the distance the auxiliary Stokeslets are spread across

the surface of the sphere from their primary Stokeslet as measured by $normPL$ (explained in greater detail in section 3.2) as the primary parameters. In the examination of the MRS, we try a simple variation (using an adaptive ϵ) to see if the error calculations can be improved. Similarly for the MARS, we use different placements of auxiliary Stokeslets and look at the impact on error. We will draw conclusions about when each method performs the best as well as the relationship between global and local error, if any.

2 Numerical Study of the Method of Regularized Stokeslets

2.1 Numerical Setup

In our numerical study, we consider a unit sphere moving in unbounded (non-dimensional) Stokes' flow. The sphere is translating with a prescribed velocity of 1 in the $\hat{\imath}$ direction with no rotational velocity. The viscosity is set to be 1. Using the MRS, we calculate the force to achieve the prescribed velocity. Each such calculation of the force is considered to be one experiment.

Using the MRS requires the discretization of the sphere into regularized point forces. We use three discretization methods (and varying numbers of points): Spherical Centroidal Voronoi Tessellations (SCVT) spheres, Box-to-Sphere (B2S) spheres, and lastly Spherical Coordinate (SC) spheres. We choose these discretizations because they represent approximately evenly spaced points (SCVT), somewhat unevenly spaced points (B2S), and very unevenly spaced points (SC). This allows us to look at the effect of Stokeslet spacing on the error. Examples of semi-spheres discretized with these methods are shown in figures 1, 2, and 3.

We want to consider spheres discretized into similar numbers of points for direct comparison between the three discretization methods. The SCVT sphere has the benefit of allowing any number of points to be used. In the B2S method, points are placed in a square grid pattern on the faces of an inscribing cube and projected onto the sphere, so the method is limited to discretizing the sphere into $N = 6 * n_{B2S}^2$ points where n_{B2S} is a natural number. In the SC method, spheres we consider are limited to $N = n_{SC}^2$ because the points are placed using sphereical coordinates and have the form: $(1, \theta_i, \varphi_j)$ where $\theta_i = \frac{2i\pi}{n_{SC}}$ and i is a non-negative integer less than n_{SC} and $\varphi_j = \frac{j\pi}{n_{SC}+1}$ where j is an integer such that $1 \leq j \leq n_{SC}$. Thus, we can never discretize a sphere into the same number of points for B2S and SC. Instead, we choose sufficiently similar numbers of points for B2S and SC.

For this paper, we always use the same radially symmetric blob function for the regularized point forces:

$$\frac{15\epsilon^4}{8\pi(|\mathbf{x}|^2 + \epsilon^2)^{\frac{7}{2}}}, \tag{12}$$

and we try varying values for the regularization parameter, ϵ. In most experiments, the same value for ϵ was used for every regularized point force in the generation of the matrix S (equation 6), with this value changing between experiments. In a few experiments, we try assigning differing values of ϵ to each regularized point force based on how much surface area of the sphere each point force represents.

Using the MRS allows us to state the problem in terms of the matrix equation 6 where $\mathbf{U}$ is a column of velocity vectors associated with the regularized Stokeslets comprising the sphere; $\mathbf{S}$ is the Stokeslets matrix which depends only on the distances between the Stokeslets, the blob choice for the regularization of the force, and the parameter ϵ; and $\mathbf{f}$ is column of force vectors associated with the Stokeslets where the force will be

scaled by the area associated with the Stokeslet. We construct $\mathbf{U}$ and $\mathbf{S}$ and use GMRES with an initial guess of zero to solve. (We note that this was due to some numerical instability in using MATLAB's built in backslash function, but a thorough examination of the numerical difficulty is beyond the scope of this thesis.)

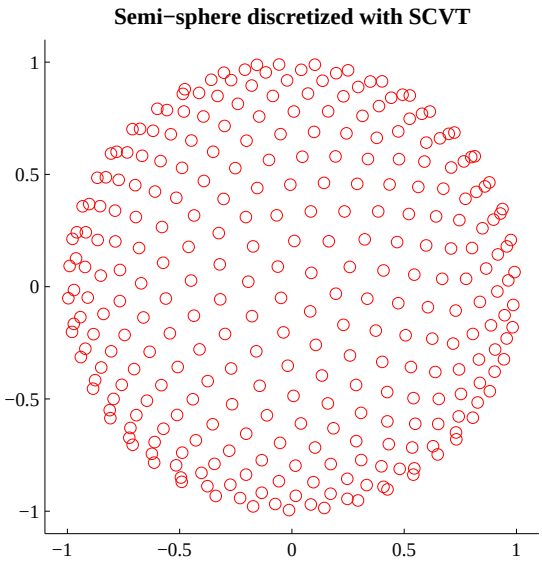

Figure 1: **SCVT Semi-Sphere** Points on the sphere are generated to form Spherical Centroidal Voronoi Tessellations (SCVT). In this plot, half of a sphere is shown head on. The points on the semi-sphere are approximately equally spaced.

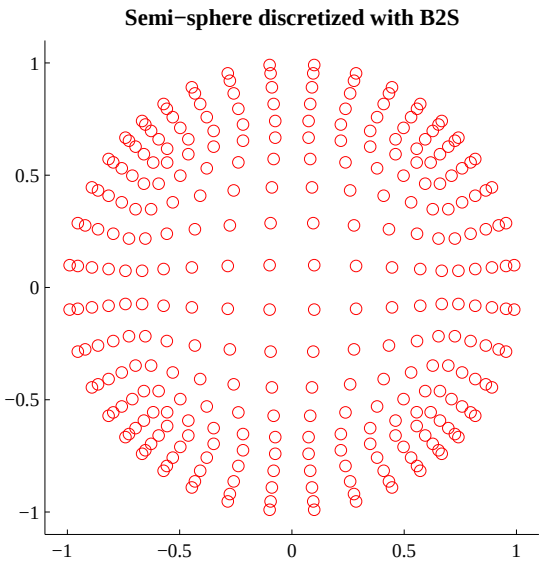

Figure 2: **Box-to-Sphere (B2S) Semi-Sphere** Sphere discretized by projecting points on an inscribing cube. The resulting points are somewhat unevenly spaced

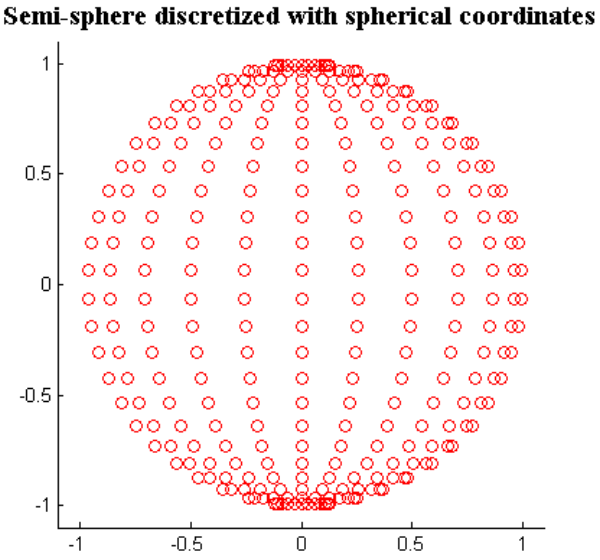

Figure 3: **Spherical Coordinate (SC) Semi-Sphere** The points generated with this method are quite unevenly spaced.

2.2 Calculated Traction Error

It is well known that the error associated with the MRS is tied to the specific choice of the parameter ϵ which controls the width of the blob (equation 12, in our case) [4, 5, 7].

As such, it is common to look at some global measure of error as it relates to the choice of ϵ in a particular test problem. Since we are prescribing velocity, we will consider traction error as our measure of global error. The traction of the sphere is known (equation 8), and we calculate the traction by summing F (equation 9) and find the associated error (equation 10).

We discretize the sphere using varying methods and different numbers of points. For each generated discretization, we vary the value of a ϵ by considering a normalized ϵ denoted E.

$$E = \frac{\epsilon}{s}, \tag{13}$$

where s is the average spacing between adjacent regularized Stokeslets. For this average, s, we use an approximation:

$$s = \sqrt{\frac{4\pi}{N}}, \tag{14}$$

where 4π is the surface area of the unit sphere, and N is the number of Stokeslets used.

Figure 4 shows the relative traction error as a function of E for our three sphere types (SCVT, B2S, and SC) with three different refinements of discretization (coarse, medium, and fine), confirming that the traction error decreases with refinement and that there is a choice of ϵ that minimizes the traction error for each discretization. This ideal ϵ is often thought to be somewhere between one-half and twice the average distance between adjacent regularized Stokeslets [8]. However, a rigorous method of choosing ϵ does not exist. Although this is problematic, we can see that the traction error does decrease as the number of points increases. For a full error analysis of the error associated with the MRS, refer to Cortez et al. [7].

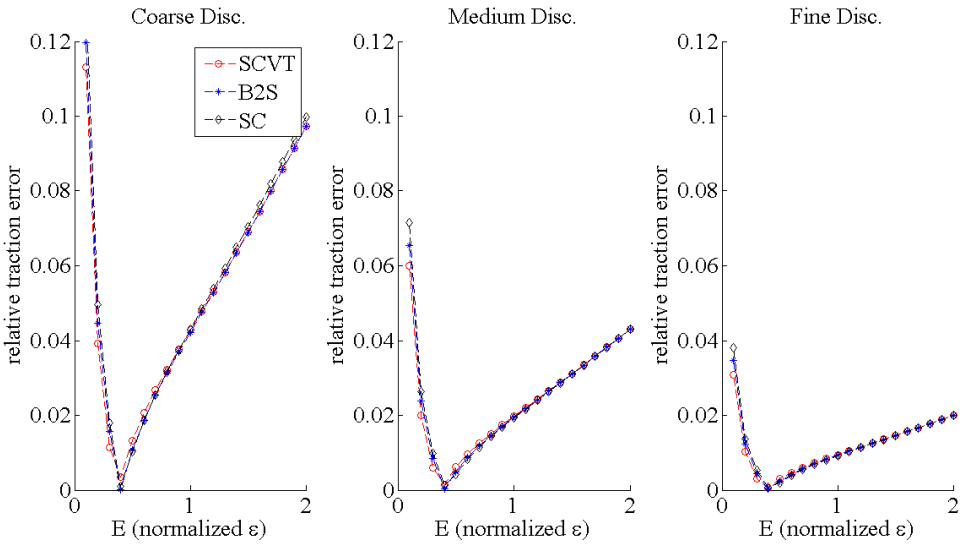

Figure 4: **MRS traction error as a function of E.** Coarse discretization: $N = 600$ (SCVT and B2S) or $N = 576$ (SC). Medium discretization: $N = 2400$ (SCVT and B2S) or $N = 2401$ (SC). Fine discretization: $N = 9600$ (SCVT and B2S) or $N = 9604$ (SC). Values are calculated for $E = 0.1$ through $E = 2$ using increments of 0.1.

From the similarity of the behavior in the traction error for all discretizations and refinements in figure 4, one might conclude that the sphere is discretization is not important for accurate force calculations and that the total number of points is the most important factor. In the next section, we will examine the local force calculations, and we will see that if we are interested in accurate local force calculations, that the total number of points, while important, is not the only factor to take into consideration.

2.3 Calculated Local Force

In this section, we look at the behavior of the force calculation locally, considering how accurate it is at each individual Stokeslet location. To do this, we choose to look at the force per unit area on a sphere. This force, $\mathbf{f}_A$ on a sphere moving in free-space Stokes' flow is analytically known to be [6]:

$$\mathbf{f}_A = \frac{3\mu\mathbf{U}}{2a}, \tag{15}$$

where $\mathbf{U}$ is the velocity of the sphere, μ is the viscosity of the fluid, and a is the radius of the sphere. It should be noted that for our sphere with a, μ, and $|\mathbf{U}| = 1$, that the exact value of $\mathbf{f}_A$ is $1.5\hat{\imath}$. By solving the matrix equation 6, we are able to find the raw force $\mathbf{f}_n$ associated with each Stokeslet. By scaling this force by the area associated with the Stokeslet, we find the associated $\mathbf{f}_{n,A}$ with equation 11. Since the velocity and force lay completely in the $\hat{\imath}$ direction, we will consider f_A as a scalar quantity of the x-component of $\mathbf{f}_A$ in the remainder of this paper. Similarly, calculated f_A (or $f_{n,A}$)is the x-component

of $\mathbf{f}_{n,A}$. The calculated f_A is compared to the analytic value of 1.5 in a qualitative way looking at graphs that show the calculated f_A values and a quantitative way by calculating the relative norm-2 f_A error:

$$Err_{norm} = \frac{\|f_{n,A} - f_A\|^2}{\|f_A\|^2}, \tag{16}$$

and the relative maximum f_A error in each experiment:

$$Err_{\max} = \max\left(\frac{|f_{n,A} - 1.5|}{1.5}\right). \tag{17}$$

For each of the three discretizations, we can calculate the area associated with every regularized Stokeslet. Spheres discretized with SCVT have the simplest algorithm. The area of each patch associated with a Stokeslet, P_A, is approximated by:

$$P_A = \frac{4\pi}{N} \tag{18}$$

where 4π is the surface area of the unit sphere, and N is the number of Stokeslets used. This formula is appropriate because the points on such a sphere are approximately equally spaced.

With B2S, using the square grid on the face of the inscribing cube, we project the cell associated with the regularized Stokeslet onto the sphere to find the corresponding area on the surface of the sphere which results in the integral formula:

$$P_A = \iint_{cell} \frac{1}{(1+u^2+v^2)^{\frac{3}{2}}}\, du\, dv, \tag{19}$$

where u and v are parameters on the cube with $u, v \in [-1, 1]$. Notice the minimum value of this integrand is $\frac{1}{\sqrt{27}}$ and the maximum value is 1. This means that as the cells of the cube become smaller (for finer discretizations) the ratio of the largest patches to the smallest patches tends towards $\sqrt{27} \approx 5.1962$: quite a difference!

Finally, for spheres that are discretized with spherical coordinates, we calculate each patch size with the integral:

$$P_A = \int_{\theta_{i-\frac{1}{2}}}^{\theta_{i+\frac{1}{2}}} \int_{\varphi_{j-k_1}}^{\varphi_{j+k_2}} \sin(\varphi)\, d\varphi\, d\theta, \tag{20}$$

where φ and θ parameterize the surface of the sphere (with a radius of 1) in spherical coordinates. Recall that $\theta_i = \frac{2i\pi}{n}$ and that $\varphi_j = \frac{j\pi}{n+1}$. We note that $k_1 = 1$ when $j = 1$ and $k_1 = \frac{1}{2}$ otherwise. Similarly, $k_2 = 1$ when $j = n$ and $k_2 = \frac{1}{2}$ otherwise. The minimum value of the integral is 0, and the maximum value is 1. This means that as the discretization of the sphere becomes finer, there is no upper limit on the ratio of the largest patches to the smallest!

Once the surface area associated with each regularized Stokeslet is known, we simply take the force we calculated from the MRS and divide by P_A to find the force per area (see equation 11). Since the sphere is moving parallel to the x-axis, we emphasize again that we only consider the x-component of the force in this calculation. Theoretically, we should not have any force in the y or z directions (see equation 15), and in the following experiments, the calculated y- and z-components of the force are orders of magnitude smaller than the x-components making them appropriate to neglect.

To efficiently examine the behavior of the calculated local force per area, we consider calculated f_A as a function of the locations of the Stokeslets. We introduce the parameter ϕ for this purpose. We define ϕ to be:

$$\phi = \arccos\left(-x_0/a\right)$$

where x_0 is the x-coordinate of Stokeslet. The angle ϕ is the angle between the negative x-axis (the x-axis is the axis of translation) and the radius of the sphere to the point.

We look at the results of our numerical experiments when the blob parameter ϵ is held fixed for each generation of the Stokeslet matrix S (equation 6)in numerical calculation of the force. Then, we examine the results of varying ϵ for the construction of S based on the surface area of the associated patch.

2.3.1 Local Force for Fixed ϵ

For all of the experiments referenced in this section, we kept ϵ constant for each generation of the Stokeslet matrix, S (equation 6), but we did not use the same ϵ for each S. Like when we calculate traction error, we consider a normalized ϵ denoted E as calculated in equation 13 using average spacing s as in equation 14.

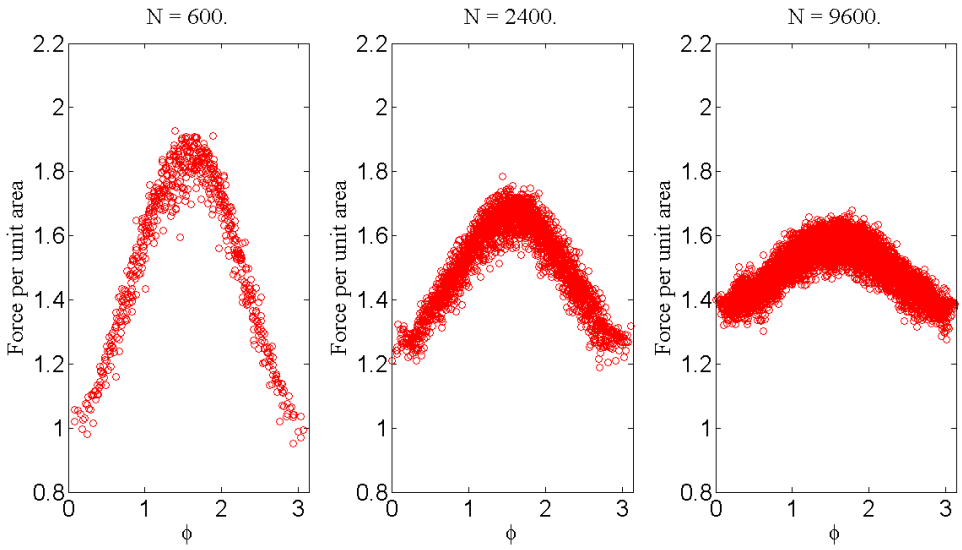

Figure 5: **MRS convergence study of Force per Area calculations for SCVT spheres.** $E = 1$ for all of the above figures. The relative traction errors of the plots from left to right are 0.0427, 0.0197, and 0.0094, and the relative maximum f_A errors from left to right are 0.3649, 0.2067, and 0.1494.

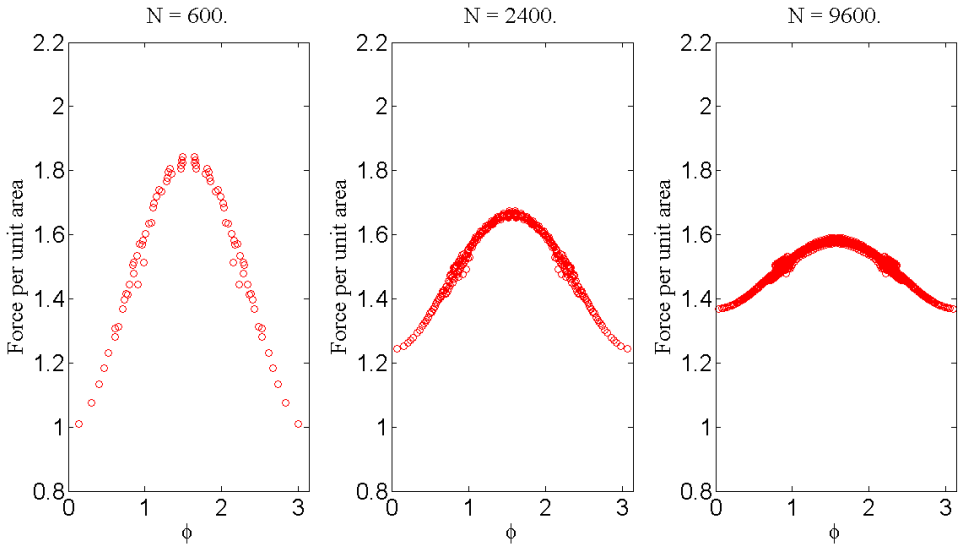

Figure 6: **MRS convergence study of Force per Area calculations for B2S spheres.** $E = 1$ for all of the above figures. The traction errors of the figures from left to right are 0.0422, 0.0195, and 0.0093, and the relative maximum f_A errors from left to right are 0.3277, 0.1710, and 0.0872.

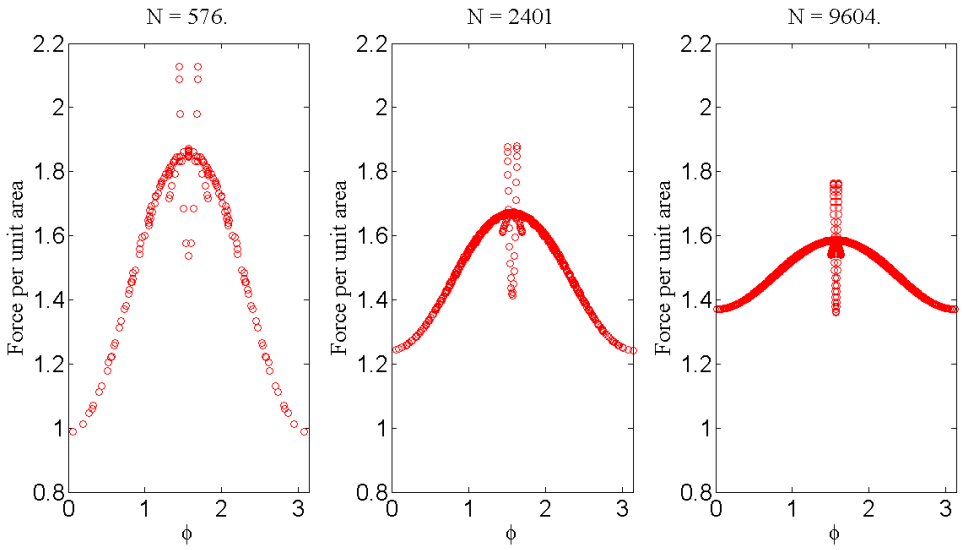

Figure 7: **MRS convergence study of Force per Area calculations for SC spheres.** $E = 1$. The traction errors from left to right are 0.0430, 0.0193, and 0.0092, and the relative maximum f_A errors from left to right are 0.4177 0.2526, and 0.1758.

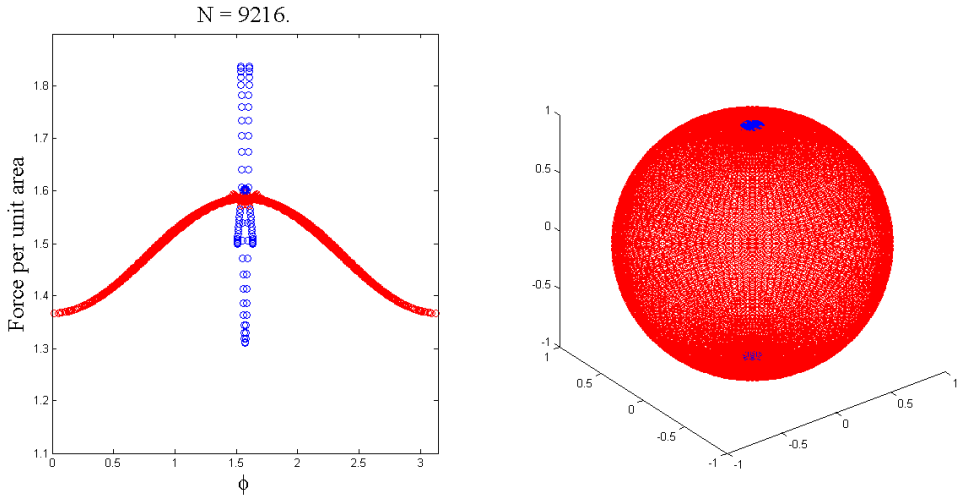

Figure 8: **Location of problematic points on a SC sphere for MRS.** The outlining points on the force curve are marked in blue on the left, and their locations on the discretized sphere are marked in blue on the right.

In figures 5, 6, and 7 we examine the convergence of the calculated force per area as we increase the number of Stokeslets, N. In the convergence study for the SCVT spheres (figure 5), we can see that as we increase the number of Stokeslets, the force per area (slowly) levels towards the true value of 1.5. It is noteworthy that for $N = 9600$ points, the

traction error is less than 1%, but the individual f_A calculations can be off by almost 15%, significantly more error. It is also notable that the configuration of points is fuzzy, but this is likely due to the assumption that P_A is exactly the same for each Stokeslet on a SCVT sphere. Even in the scenario of evenly spaced points, the f_A error can be almost 15 times the traction error.

The next convergence study is of the B2S discretization (figure 6). Like the SCVT study, the force curve is slowly tending towards 1.5 as we increase the number of points. There are subtly outlying points from the curve that are notable and correspond to the location of the corners of the inscribing cube; they correspond to where the regularized Stokeslets are closest together. Although we generally see better behavior than we did with the SCVT spheres, the f_A error can still be more than 8 times the traction error.

The last convergence study on f_A was performed for the SC discretization (figure 7). While most of the points along the force curve for this discretization are converging to 1.5 as we increase the number of points, many points near $\phi = \frac{\pi}{2}$ do not converge as the discretization becomes finer. These problem points are near the poles. Figure 8 shows exactly where the non-converging points are for a sphere with $N = 9216$ points.

There are two important conclusions from these convergence studies. The first is that even when the f_A calculations are well-behaved as in figure 6, the f_A error can be significantly bigger than the traction error. The second important conclusion is that patches of densely clustered points can cause major, local problems in the calculation of f_A.

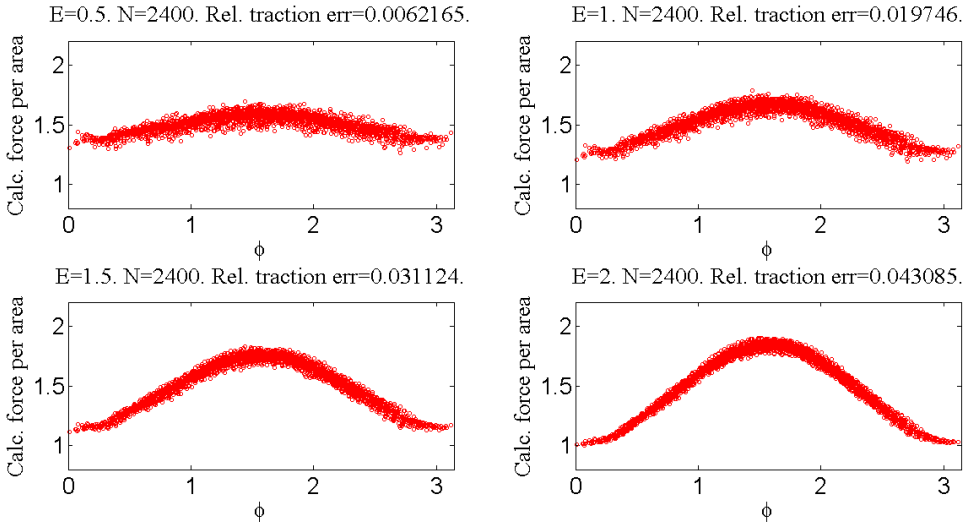

Figure 9: **MRS Calculated Force per Area on a 2400 point SCVT sphere with Varying E.**

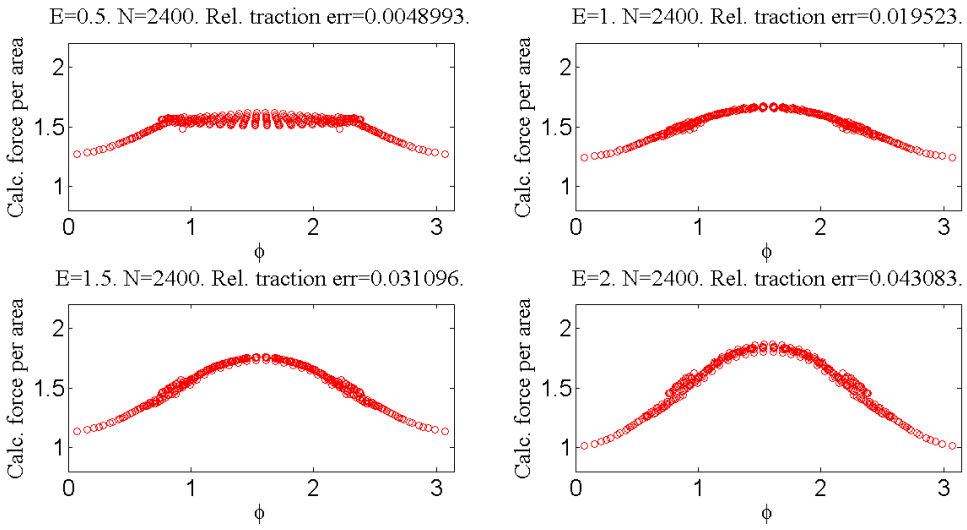

Figure 10: **MRS Calculated Force per Area on a 2400 point B2S sphere with Varying E.**

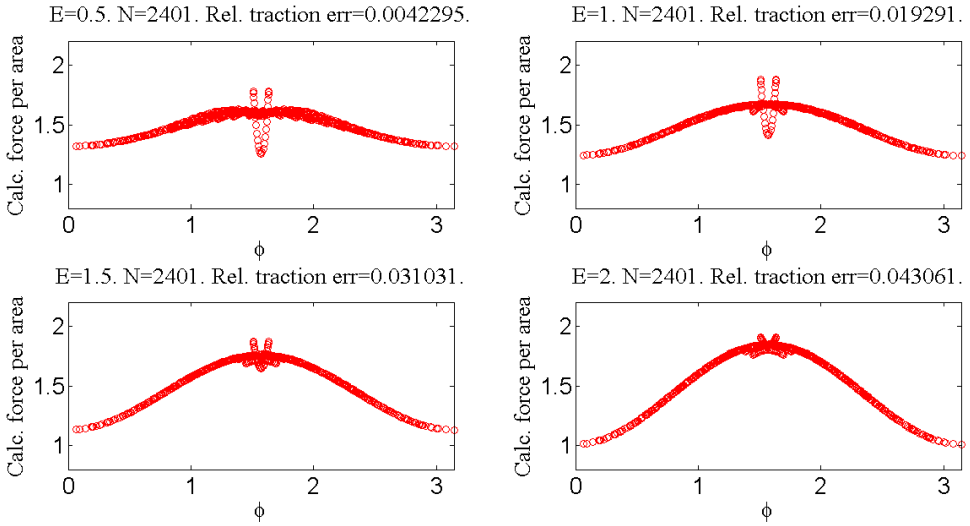

Figure 11: **MRS Calculated Force per Area on a 2401 point SC sphere with Varying E.**

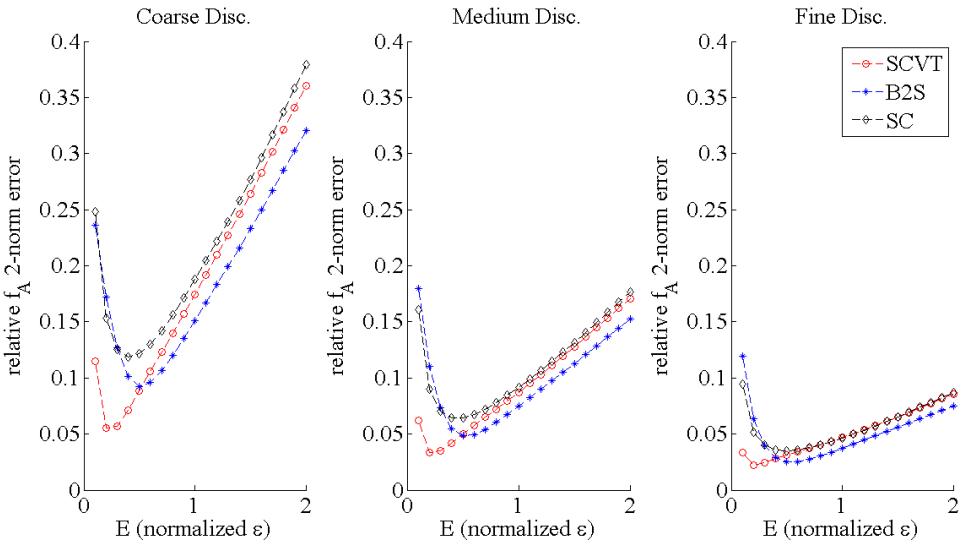

Figure 12: **MRS Relative f_A Norm-2 Error as a Function of E.** Values are calculated for $E = 0.1$ through $E = 2$ in increments of 0.1.

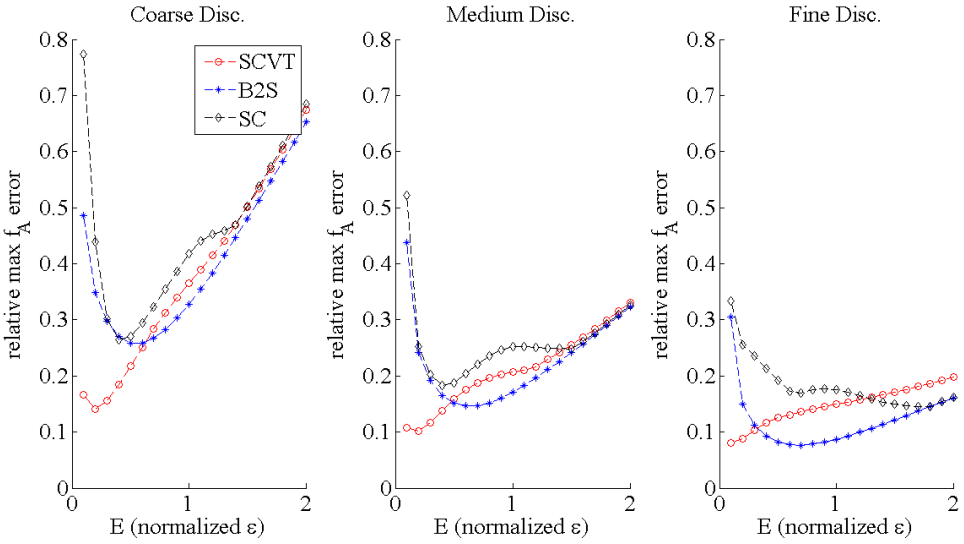

Figure 13: **MRS Relative Maximum f_A Error as a Function of E.** Values are calculated for $E = 0.1$ through $E = 2$ in increments of 0.1.

We explore this further by looking at the qualitative behavior of the f_A calculations for medium refinement spheres for four different values E in figures 9, 10, and 11 for the SCVT, B2S and SC spheres respectively. To quantify the effect of E on the local force curves, we consider relative f_A norm-2 error (equation 16) and relative maximum error (equation 17) as functions of E for three different refinements of SCVT, B2S, and SC spheres in figures 12 and 13 respectively.

Taken together, we see that overall the force calculations look similar for each value of E no matter which discretization type we use (figures 9, 10, and 11) which is quantified by similar values of relative f_A norm-2 errors across all sphere discretizations for each refinement (for E in the typical range of 0.5 to 2) in figure 12. We also notice that the discretization type can have a noticeable effect on the relative maximum f_A error in figure 13. Our force calculations on the SC sphere (figure 11) tells us the maximum error is located where points are clustered together. Also, our force calculations on the SCVT sphere (figure 9) suggest its somewhat higher maximum f_A error compared to the B2S sphere (figure 10) is not a result of clustered points but likely a result of the overall fuzzy appearance of the SCVT sphere's f_A, possibly due to the inaccuracy of representing each Stokeslet on the SCVT sphere as having the same area.

We conclude the discretization type can significantly affect the relative maximum f_A error and ϵ has a larger effect on the local errors than it does on the global error; there is a larger range of values for the relative f_A norm-2 error and relative maximum f_A errors for the same values of E than there is for the relative traction error. The relationship between these three errors is explored further in section 2.4.

2.3.2 Local Force for Adaptive ϵ

After seeing the non-smooth behavior of the force calculation in figure 11 and to a much lesser extent figure 10, we consider a potential solution to the problem involving varying the blob parameter, ϵ, value associated with each Stokeslet for a single calculation of the Stokeslet matrix S (equation 6). We still consider a normalized E as in equation 13 but calculated via:

$$s = \sqrt{P_A},$$

where P_A is the surface area associated with a particular Stokeslet. Thus, we could still consider a constant ratio of ϵ to s for every regularized Stokeslet within a calculation while having a different ϵ associated with each individual Stokeslet within the calculation.

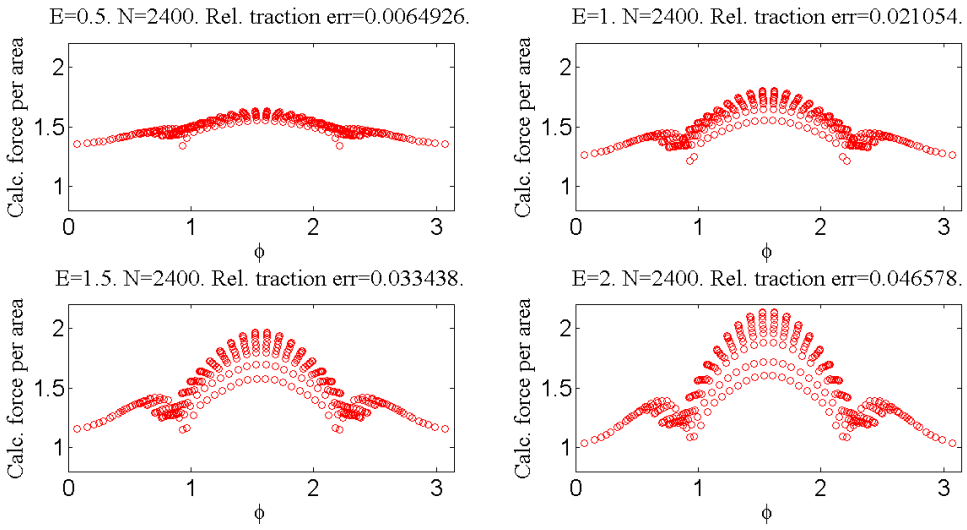

Figure 14: **MRS Calculated Force per Area on a 2400 point B2S sphere with adaptive ϵ.**

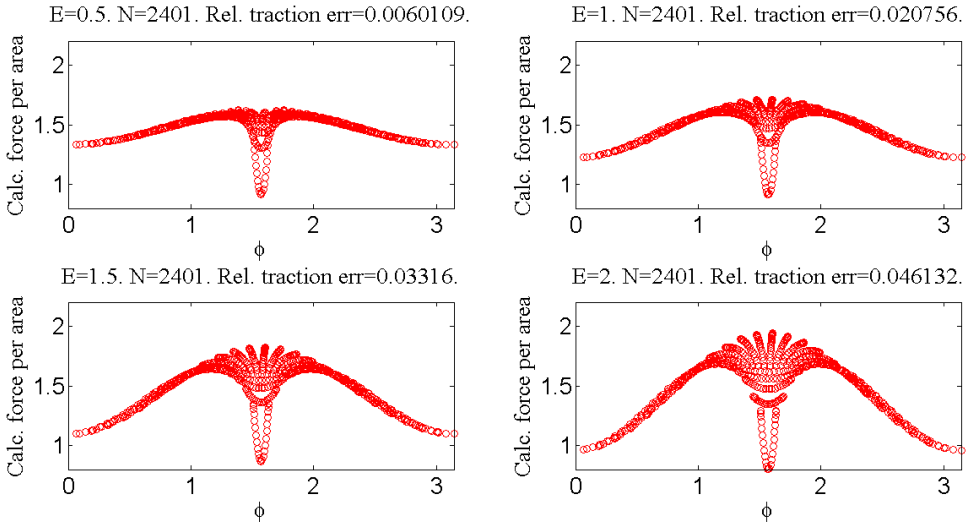

Figure 15: **MRS Calculated Force per Area on a 2401 point SC sphere with adaptive ϵ.**

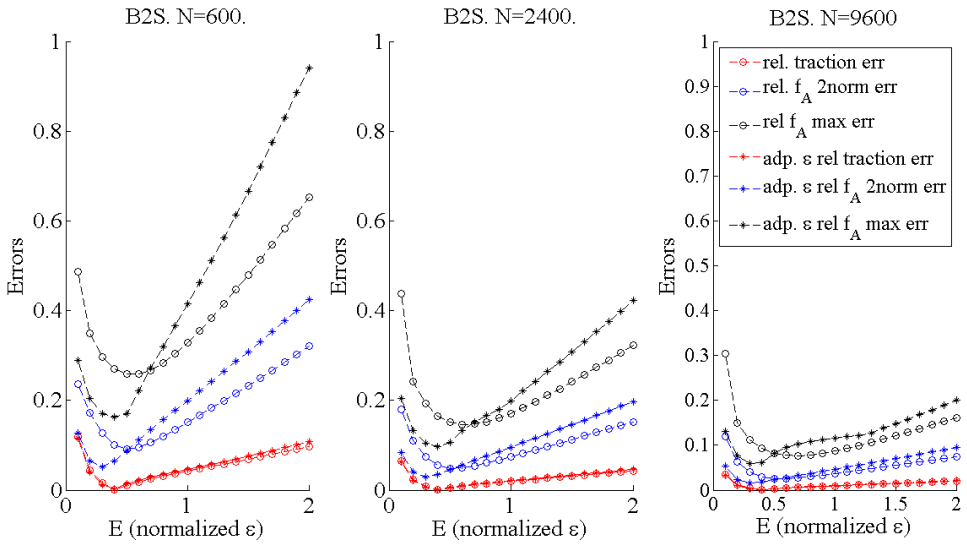

Figure 16: **Comparison of Errors for Adaptive and Non-Adaptive ϵ on B2S spheres.** Values are calculated for $E = 0.1$ through $E = 2$ in increments of 0.1.

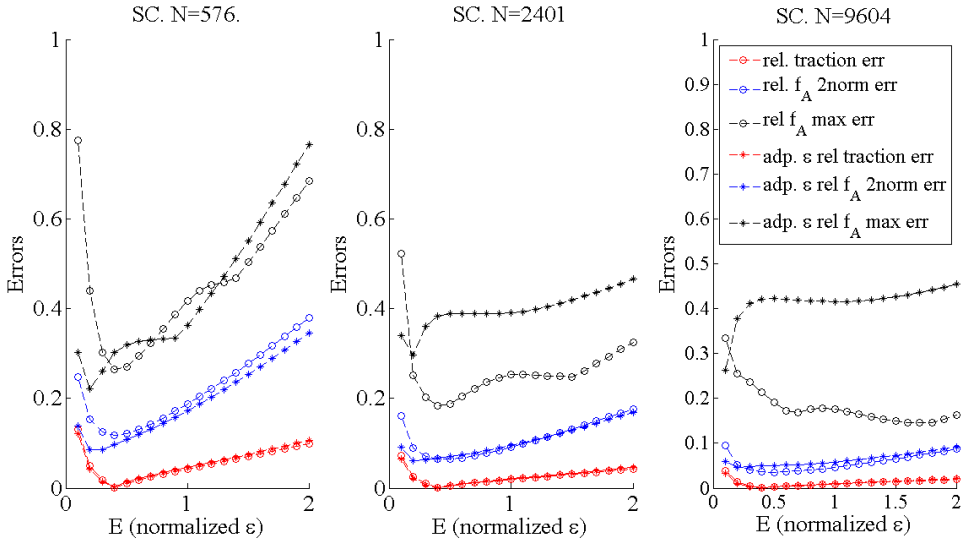

Figure 17: **Comparison of Errors for Adaptive and Non-Adaptive ϵ on SC spheres.** Values are calculated for $E = 0.1$ through $E = 2$ in increments of 0.1.

The results of repeating the force calculations of figures 10 and 11 with a varying ϵ are seen in figures 14 and 15. Qualitatively, the results of using an adaptive ϵ to contruct the Stokeslet matrix, S, do not look better than the original force calculations. We compare all error calculations (relative traction, f_A norm-2, and max f_A errors) for adaptive and non-adaptive ϵ as a function of E for B2S spheres in figure 16 and SC spheres in figure 17. In the case of B2S, the error is generally similar for non-adaptive and adaptive ϵ with the adaptive

ϵ technique giving somewhat worse error in the usual E range of 0.5 to 2. However, in the case of the SC sphere, the relative maximum f_A error is significantly worse with adpative ϵ for medium ($N = 2401$) and fine ($N = 9604$) refinements. Using an adaptive ϵ does not smooth the problematic points, or at least, adapting ϵ in such a simple way does not. Although trying an adaptive ϵ seems a natural solution, it does not improve results. Further investigation is merited in the future.

2.4 Global and Local Error Comparison

In this section, we consider the relationship between the global and local error calculations. In the previous sections, we discuss global traction error, local f_A norm-2 error, and maximum f_A error, and their relationship to the blob parameter, ϵ. We see that often when the traction error was small, that the f_A errors is much bigger.

In figure 18, we examine the relationship of local and global error. Specifically, we examine the relationship of the relative f_A norm-2 error to the relative traction error and the relationship of the relative maximum f_A error to the traction error for values of E from 0.5 through 2. Although a thorough statistical analysis has not been performed, there is compelling graphical evidence that the f_A errors correlate strongly with traction error, especially when non-adaptive ϵ is used. The plots also reinforce our earlier finding that the f_A (maximum or norm-2) error can be much greater than the traction error. Since there is evidence of a direct relationship, further future analysis and investigation is merited.

In figure 19, we confirm that as the number of Stokeslets increases, and therefore the average spacing, s, between Stokeslets decreases (see equation 14), all the error measures decrease with the sole exception of the maximum f_A error for the SC sphere with adaptive ϵ. However, using an adaptive ϵ is not the standard choice for this method, and this result lends further evidence to support that such a simply adaptive ϵ should not be used. We note errors appear to depend linearly on s as expected for calculations on the surface when regularization error is dominate [7].

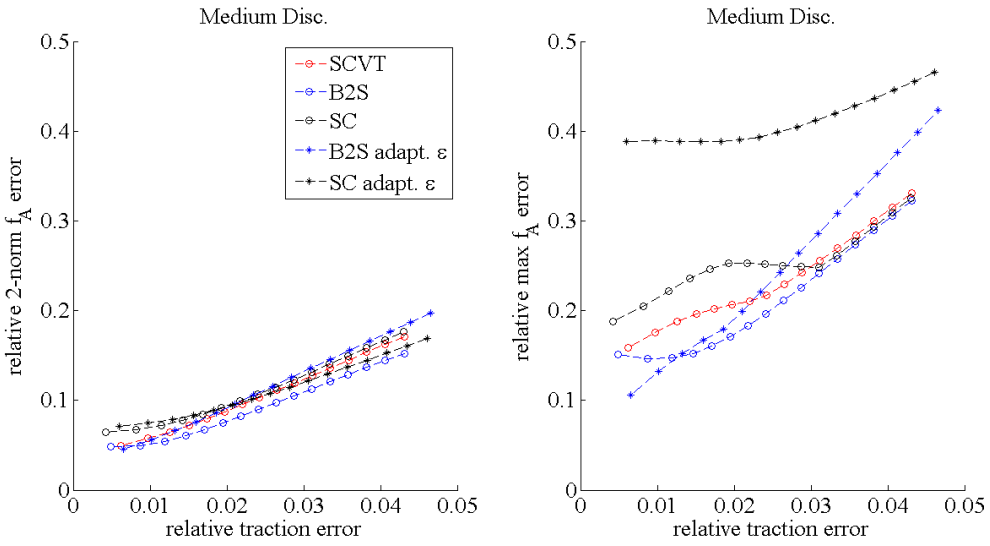

Figure 18: **MRS: Comparison of Local and Global Errors**

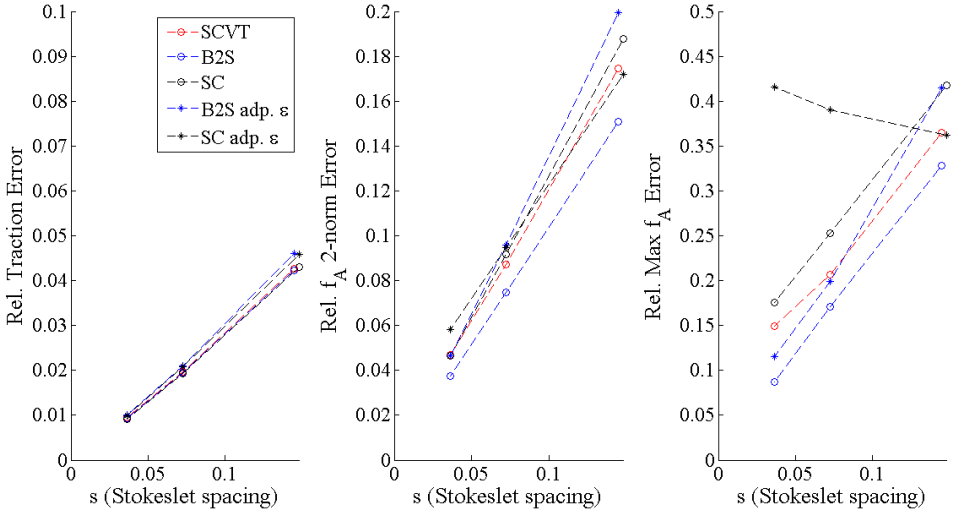

Figure 19: **MRS: Local and Global Errors as a Function of Stokeslet Spacing, s.** As N, the number of primary Stokeslets increases, s decreases. $E = 1$ for all calculations shown.

3 Numerical Study of the Method of Auxiliary Regularized Stokeslets

3.1 Numerical Setup

We now consider the Method of Auxiliary Regularized Stokeslets (hereafter referred to as MARS) [5] with the setup for the numerical experiments as in chapter 2. That is, we consider a sphere translating with unit velocity in unbounded Stokes' flow and calculate the force required to maintain motion.

Like the MRS, the MARS requires the discretization of the sphere into regularized Stokeslets. Now though, two types of Stokeslets are considered: primary Stokeslets and auxiliary (or fictitious) Stokeslets. The primary Stokeslets are the same Stokeslets as in the normal MRS. Auxiliary Stokeslets are placed around each primary Stokeslet, more finely discretizing the surface of the sphere, and their purpose is to more accurately capture the effect of each Stokeslet on itself; when we must calculate the effect of the Stokelet on its own location, we don't use the primary Stokeslet like we do in the MRS. Instead, we use an average of the effects of the auxiliary Stokeslets on the location of the primary Stokeslet (see equation 7). All other calculations are the same as in the MRS; when we consider any location away from our primary Stokeslet, we use the primary Stokeslet to calculate the effect. That is the MARS, like the MRS, allows us to state the problem to find the forces in a matrix equation 6 where the diagonal entries in $\mathbf{S}$ that reflect the effect of a Stokeslet on itself are modified. Like the previous section, here all matrix solves are done with GMRES.

Having both primary Stokeslets and auxiliary Stokeslets means we must consider two separate discretizations: one for the primary Stokeslets and one for the auxiliary Stokeslets. We choose the same discretizations for the primary Stokeslets in the study of the MARS as we did in the study for the MRS. For the auxiliary Stokeslets, we consider two possibilities. One is to use approximately square patches (abbreviated as Sq. patches in this paper) of auxiliary Stokeslets. The other is to use the underlying discretization of the primary Stokeslets to create a finer grid of auxiliary Stokeslets around each primary Stokeslet. These various dual discretizations are illustrated in figures 20, 21, and 22; these figures show the five situations we consider. It should be noted that for the SCVT sphere, we only consider Sq. patches since the discretization is approximately evenly spaced.

In the MARS, we use the same blob function as in equation 12 that we use in the MRS. For each calculation of the matrix $\mathbf{S}$ in equation 6, every Stokeslet (auxiliary or primary) uses the same blob function with the same value of the parameter ϵ. Furthermore, ϵ was chosen based on the spacing of the **auxiliary** Stokeslets, not the primary Stokeslets. For all of the calculations in this paper, we used 121 auxiliary Stokeslets for each primary Stokeslet. (Figures 20, 21, and 22 only show 25 auxiliary Stokeslet per primary Stokeslet in order to more clearly show the pattern of placement.) Only 121 are used due to previous experimental numerical work that shows diminishing returns as the number of auxiliary Stokeslets is increased.

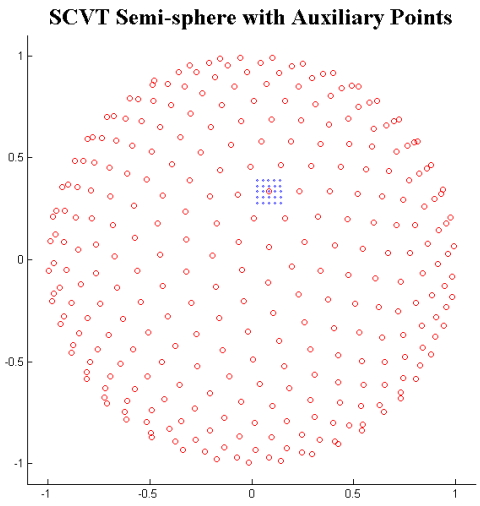

Figure 20: **SCVT Semi-Sphere with Auxiliary Stokeslets shown for single Primary Stokeslet**

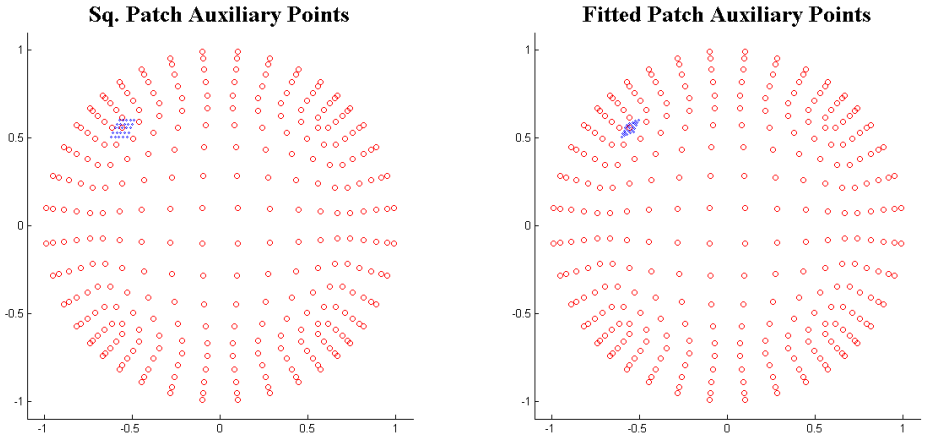

Figure 21: **Box-to-Sphere (B2S) Semi-Sphere with two different placements of Auxiliary Stokeslets** On the left, auxiliary Stokeslets are placed to form an approximately square patch (Sq. patch). On the left, Stokeslets are placed to match the discretization of the sphere.

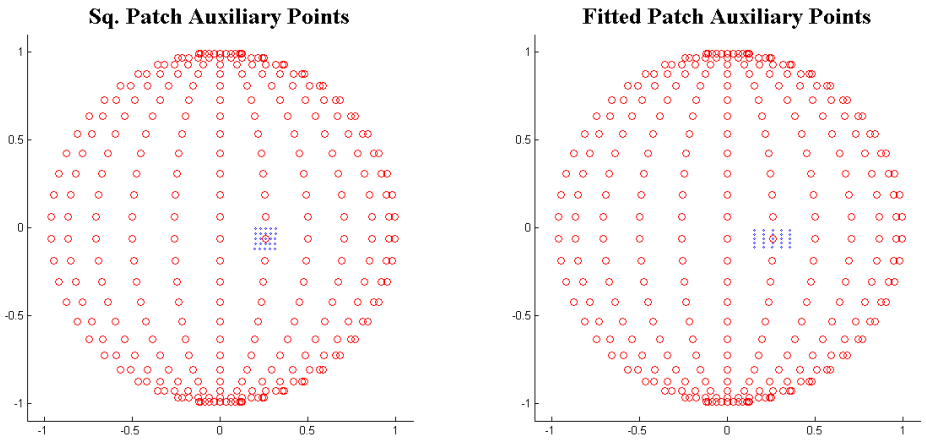

Figure 22: **Spherical Coordinate (SC) Semi-Sphere with two different placements of Auxiliary Stokeslets** On the left, auxiliary Stokeslets are placed to form an approximately square patch (Sq. patch). On the left, Stokeslets are placed to match the discretization of the sphere.

3.2 Calculated Traction Error

Similar to the MRS, traction error is used as a first measure of performance of the MARS, in the next subsections the traction error is shown as a function of the number of **primary** Stokeslets, N; normalized ϵ, E; and normalized patch length, $normPL$. The results are broken up into two sections: one focusing on the effect of E and another that focuses on the effect of $normPL$. These are all parameters that we can control in the application of the MARS, and we wish to know which are the most influential and how they affect the global error. Later we will examine their effects on the calculation of the local forces.

The parameter E is calculated similarly to equation 13, but we now normalize by the average spacing of the auxiliary Stokeslets:

$$E = \frac{\epsilon}{s_{aux}},$$

$$s_{aux} = \sqrt{\frac{4\pi}{121N}},$$

where 4π is the surface area of the sphere and 121 is the number of auxiliary Stokeslets per primary Stokeslet.

Normalized patch length only applies to discretizations with Sq. patches. Patch length refers to the approximate side length of each Sq. patch, and this length, L is divided

by the average spacing between primary Stokeslets (equation 14) to acheive $normPL$:

$$normPL = \frac{L}{s}.$$

3.2.1 Traction Error as a Function of E

One of Barrero-Gil's central arguments for implementation of the MARS over the MRS is that the MARS weakens the dependence of the traction error on the parameter E [5]. In figure 23 the relative traction error is small in all cases (generally less than 1%), regardless of the choice of E. The errors for typical E values between $E = 0.5$ and $E = 2$ are similar with an absolute difference of about 0.5% in the worst case for a coarsely discretized sphere. Compared to the MRS, where the error values (see figure 4) can have an absolute difference of more than 8% for the coarsely discretized spheres. And for all cases, the difference in error between $E = 0.5$ and $E = 2$ is an about an order of magnitude less using the MARS versus the MRS! Furthermore, this pattern holds whether we use Sq. patches or Fitted patches.

As the number of primary Stokeslets increases, the relative traction error decreases showing that the traction calculations using the MARS converge similarly to using the MRS: as N approximately quadruples, the relative traction error is cut about in half.

From the small traction errors, one might be misled to conclude that the discretization of the sphere does not matter as the errors are similar across all results that share similar values of N no matter the discretization of the primary and auxiliary Stokeslets, and that E truly does not have a strong effect on the results. However, from the previous study of the MRS in this paper, we know that small traction error does not necessarily provide a good indication of the behavior of the force on the local level. We will examine this later in the paper, and the good results seen here make the further investigation worthwhile.

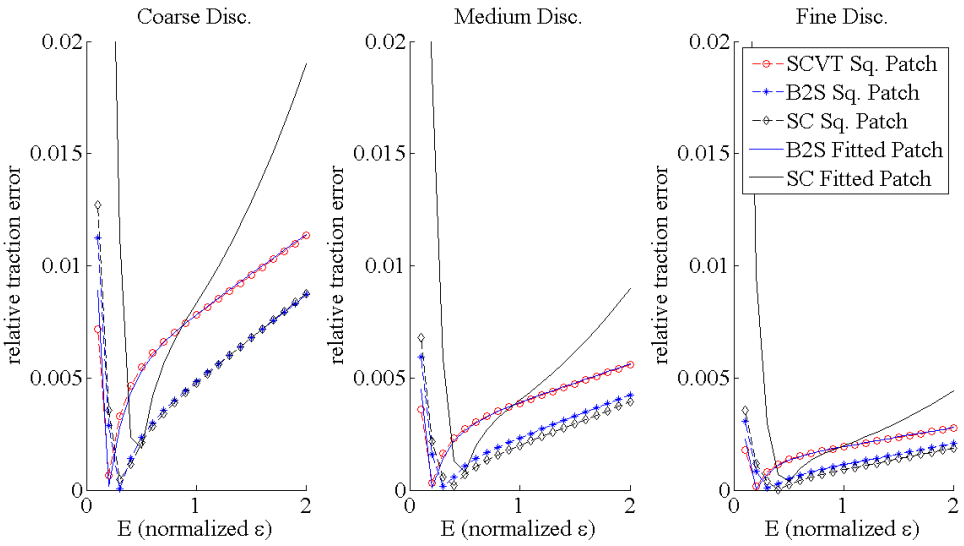

Figure 23: **MARS traction error as a function of** E Coarse discretization: $N = 600$ (SCVT and B2S) or $N = 576$ (SC). Medium discretization: $N = 2400$ (SCVT and B2S) or $N = 2401$ (SC). Fine discretization: $N = 9600$ (SCVT and B2S) or $N = 9604$ (SC). Values are calculated for $E = 0.1$ through $E = 2$ using increments of 0.1.

3.2.2 Traction Error as a Function of $normPL$

Now we consider the spread of the auxiliary Stokeslets by considering the parameter $normPL$ which measures the normalized patch length. It should be noted that we only consider $normPL$ between 0.1 and 2 due to increasing numerical instability involved in solving the matrix system 6 as $normPL$ increases. (The examination of the exact cause of this instability merits further investigation, but is beyond the scope of this thesis.) If we consider L as the length of our approximately square patch of auxiliary Stokeslets, then:

$$normPL = \frac{L}{s},$$

where s is the average spacing between **primary** Stokeslets (see equation 14).

Figure 24 shows the traction error on the sphere as we vary $normPL$. All three discretizations of the sphere involving Sq. patches show extremely similar error. The plots show that traction error is minimized when $normPL$ is slightly less than 1. This makes intuitive sense as the auxiliary Stokeslets capture the effect of the Stokeslet on itself, and a $normPL$ of about 1 represents the amount of surface (on average) the Stokeslet is supposed to represent; it doesn't make sense to have auxiliary Stokeslets as far away as other primary Stokeslets (like is the case with $normPL = 2$) because such placement would count the effect of part of the surface of the sphere on the location of the primary Stokeslet twice: once in the averaging of the auxiliary Stokeslets' effect and once again in the effect of another primary Stokeslet. Also, if the auxiliary points are too close to the

primary Stokeslet, we are moving back towards the case of the MRS and not making good use of their effect. We will examine the effect of $normPL$ further when we look at the local force calculations for the MARS.

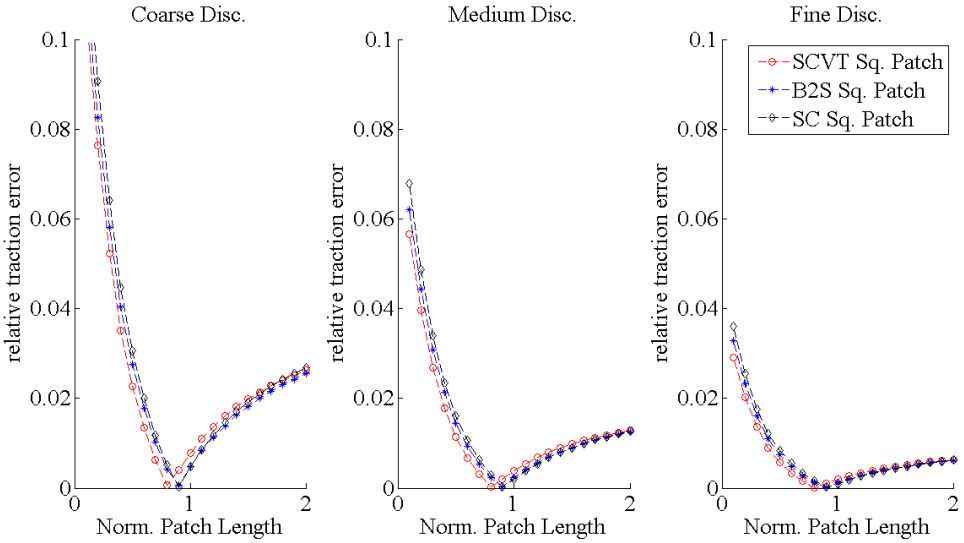

Figure 24: **MARS Traction Error as a Function of $normPL$.** Coarse discretization: $N = 600$ (SCVT and B2S) or $N = 576$ (SC). Medium discretization: $N = 2400$ (SCVT and B2S) or $N = 2401$ (SC). Fine discretization: $N = 9600$ (SCVT and B2S) or $N = 9604$ (SC). Values are calculated for $normPL = 0.1$ through $normPL = 1.5$ using increments of 0.1.

3.3 Calculated Local Force

In order to understand how the MARS performs on a local level we look at the force per area, f_A, calculations just as we did for the MRS. Once the Matrix equation 6 is solved for $\mathbf{f}$, the force per area calculations are performed exactly as detailed previously for the MRS using equation 11 and equation 18, 19, or 20 as appropriate. Again, we consider both qualitative and quantitative measures of the behavior of the f_A calculation by viewing the behavior of f_A plots and measuring the relative f_A norm-2 error and the relative maximum f_A error.

In the next two sections, we look at the influence of the number of primary Stokeslets, N; the normalized blob parameter, E; and the normalized patch length, $normPL$ on the f_A calculations and the associated relative f_A norm-2 and maximum f_A errors. We break our analysis up into one section that focuses on E and one that focuses on $normPL$ while considering the effects of N in each. Our aim is to understand the effects of the parameters N, E, and $normPL$ on the f_A calculation and draw some conclusions about the best discretization to use in terms of the associated error.

3.3.1 Local Force as a Function of E

In the traction error calculations, we saw that the normalized blob parameter, E, did not play as much of a role for the MARS as it did with the MRS. Here we explore whether this is not only the case for the traction error calculations but also for the f_A calculations as well. We look at this qualitatively by seeing if the general f_A calculations change significantly as E is changed (see figures 27 through 31). (We see that the force calculations look generally the same as E is changed.) Quantitatively, we examine the relative f_A norm-2 error as well as the relative maximum f_A error as functions of E for varying N in figures 25 and 26 respectively.

In figures 25 and 26, we see that both measures of the local (the norm-2 and maximum) error of some discretizations (SCVT with Sq. Patches, and B2S with Sq. or Fitted Patches) vary little as E changes in the typical range of 0.5 to 2. The relative maximum f_A error remains high for the SC with Sq. Patches or SC with Fitted Patches discretizations, and these errors vary significantly as E changes. The plots of f_A for the SC spheres in figures 29 and 31 clarify that this poor behavior of the relative maximum f_A error is linked to clustered points on the sphere. However, 25 shows that the norm-2 error varies little as a function of E. This means that the general closeness of the f_A calculations to the true value is largely not changing as a function of E, so we are satisfied that E has a relatively weak effect on the overall f_A calculation.

We will not attempt to quantify at this stage which discretization is the best as we still must consider the effect of $normPL$ on the discretizations that use Sq. Patches. However, we already see that the SC discretization causes issues not present in SCVT or B2S.

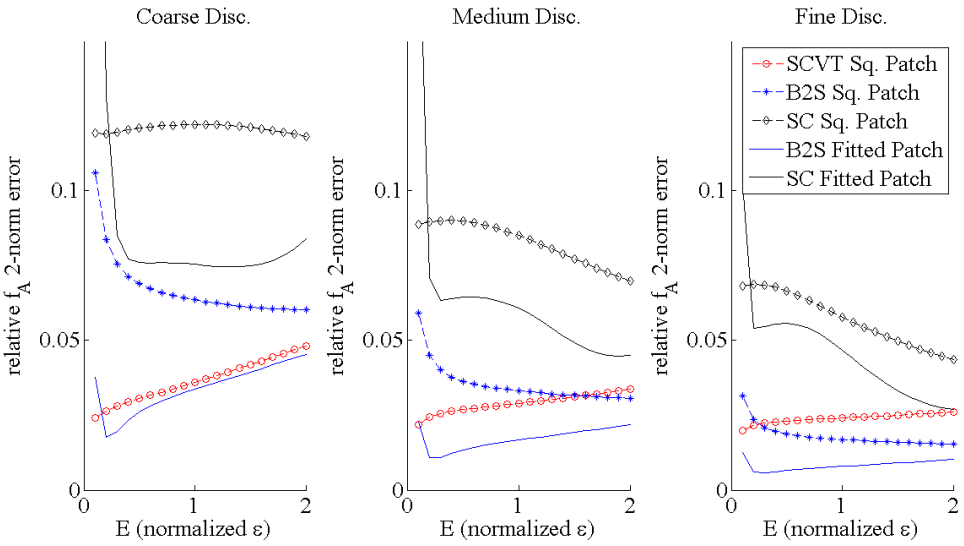

Figure 25: **The Relative f_A 2-norm Error as a Function of E.** Coarse discretization: $N = 600$ (SCVT and B2S) or $N = 576$ (SC). Medium discretization: $N = 2400$ (SCVT and B2S) or $N = 2401$ (SC). Fine discretization: $N = 9600$ (SCVT and B2S) or $N = 9604$ (SC). Values are calculated for $E = 0.1$ through $E = 2$ using increments of 0.1.

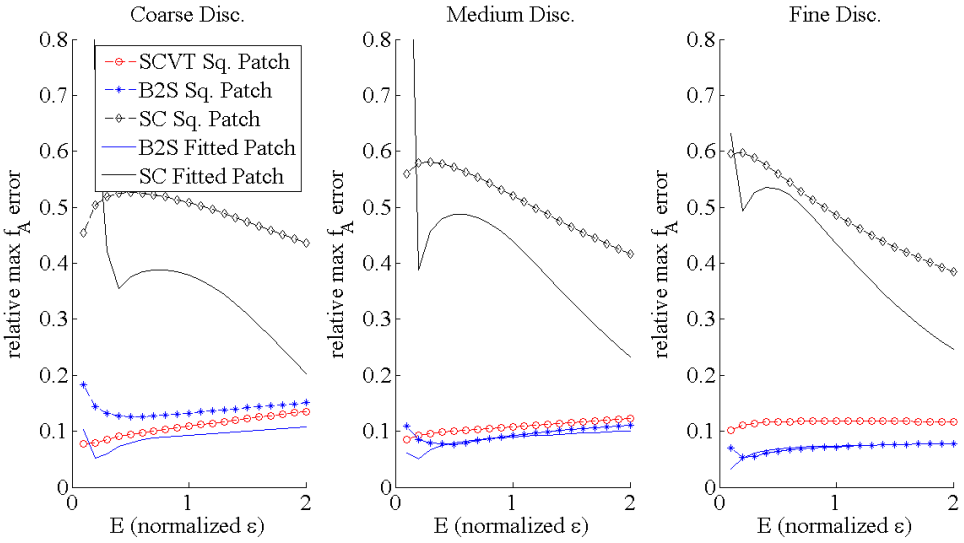

Figure 26: **The Relative Maximum f_A Error as a Function of E.** Coarse discretization: $N = 600$ (SCVT and B2S) or $N = 576$ (SC). Medium discretization: $N = 2400$ (SCVT and B2S) or $N = 2401$ (SC). Fine discretization: $N = 9600$ (SCVT and B2S) or $N = 9604$ (SC). Values are calculated for $E = 0.1$ through $E = 2$ using increments of 0.1.

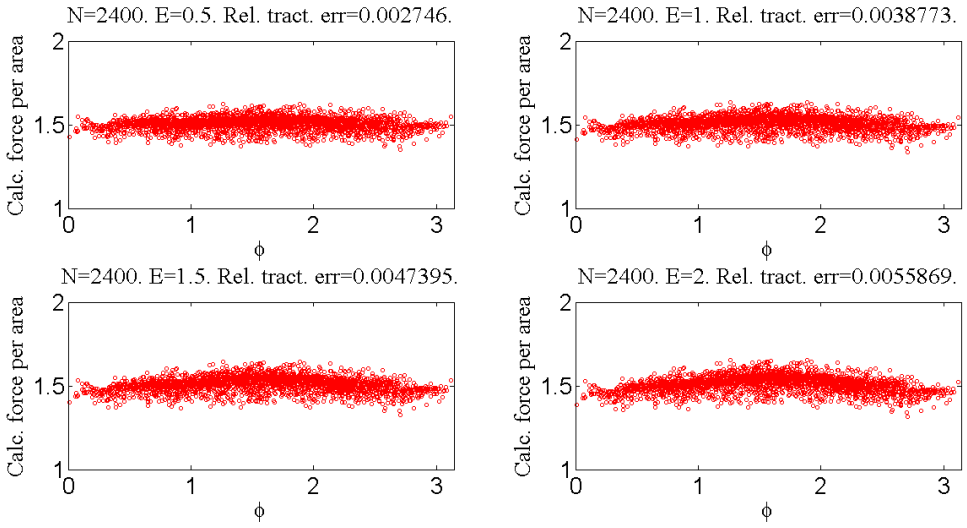

Figure 27: **MARS Force per Area results for a SCVT sphere with 2400 points, Sq. Patches, and Varying E.**

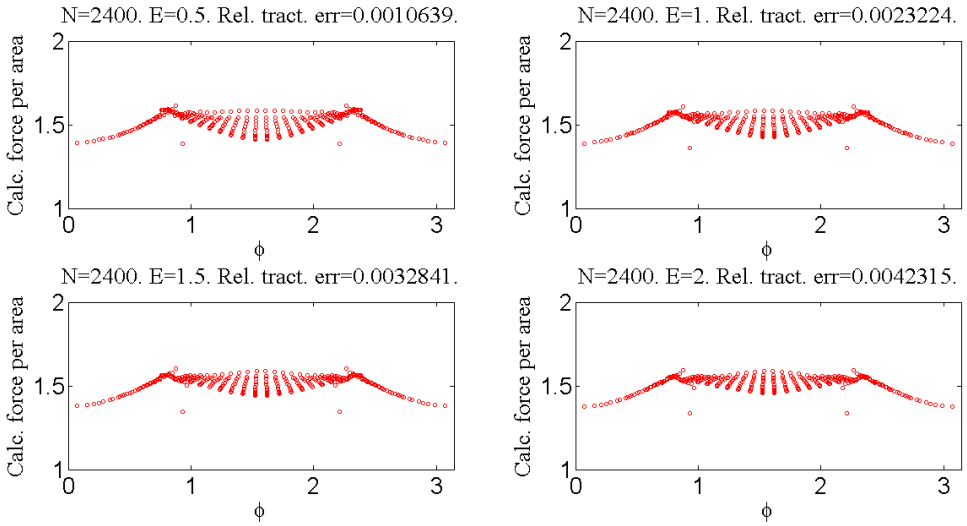

Figure 28: **MARS Force per Area results for a B2S sphere with 2400 points, Sq. Patches, and Varying E.**

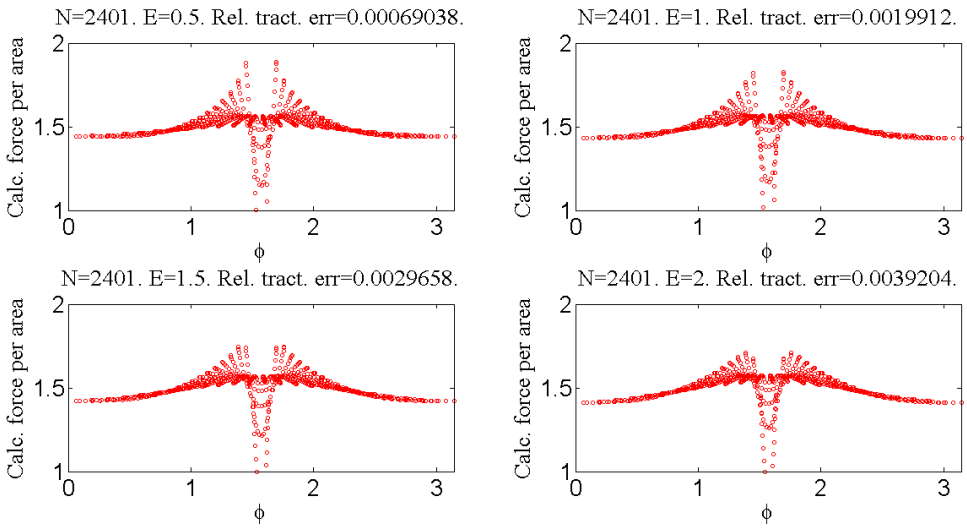

Figure 29: **MARS Force per Area results for a SC sphere with 2401 points, Sq. Patches, and Varying E.**

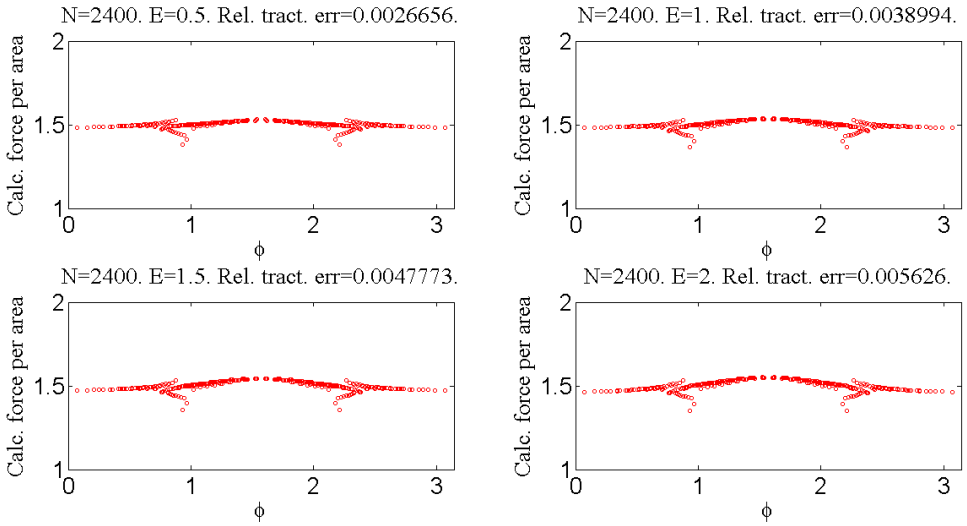

Figure 30: **MARS Force per Area results for a B2S sphere with 2400 points, Fitted Patches, and Varying E.**

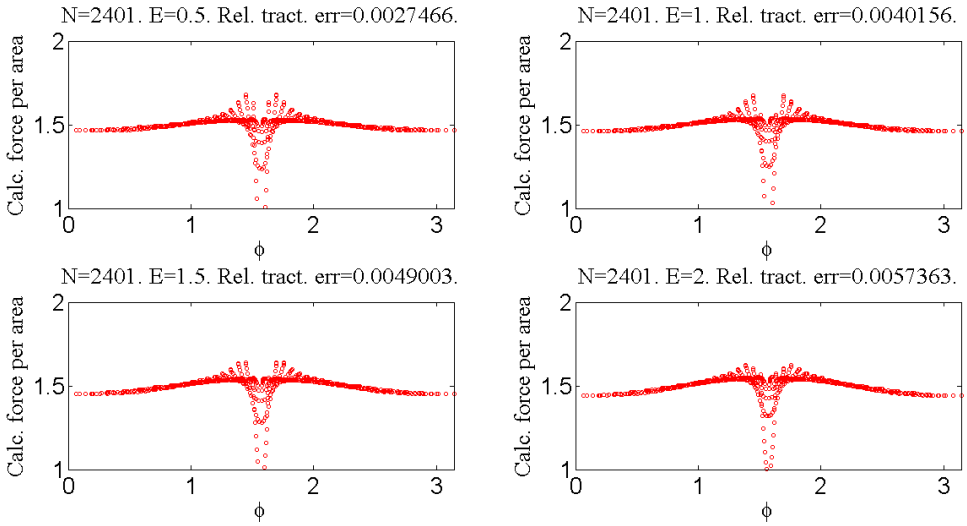

Figure 31: **MARS Force per Area results for a SC sphere with 2401 points, Fitted Patches, and Varying E.**

3.3.2 Local Force as a Function of $normPL$

When the discretization of the sphere uses Sq. Patches, we consider the parameter $normPL$, which measures how far the auxiliary Stokeslets are spread from their primary Stokeslet compared to the spacing between primary Stokeslets. Examining the effect of $normPL$ on the results of f_A in figures 34, 35, and 36 for different discretizations of the sphere (at a medium refinement) shows us that $normPL$ has an important effect.

Examining the relative f_A norm-2 error in figure 32 and the relative maximum f_A error in figure 33 shows us the SC consistently performs poorly compared to the other options available. Furthermore, when we consider that $normPL$ should be around 1 to minimize the traction error (figure 24), we can see that for the coarsest refinement, SCVT provides the best results both for relative f_A norm-2 error and relative maximum f_A error. For a medium refinement, SCVT and B2S perform similarly in terms of both errors for $normPL$ near 1. However, the relative maximum f_A error is less dependent on $normPL$ for the SCVT sphere. This suggests that the SCVT is the best choice for Sq. Patches with a coarse or medium refinement. Since one motivation to use the MARS is to use fewer primary Stokeslets than the MRS so that the matrix S is smaller and the equation 6 is easier to solve, this means that when using Sq. Patches, SCVT with a coarse refinement is usually the best choice.

Figure 34 shows the force calculation for the medium refinement SCVT sphere as $normPL$ is varied. The fuzzy appearance of f_A again suggests that we are not dividing by the proper area (P_A in equation 11), and that we could improve the f_A calculations further by more accurately calculating the area represented by each primary Stokeslet, which might lead to universally better results in the error calculations compared to SC and B2S.

In the f_A calculations for the B2S and SC spheres (figures 35 and 34) we can see where the maximum error occurs. For both discretizations the maximum error corresponds to where primary Stokeslets are the most closely clustered. This means more caution should be used the more unevenly discretized the sphere is.

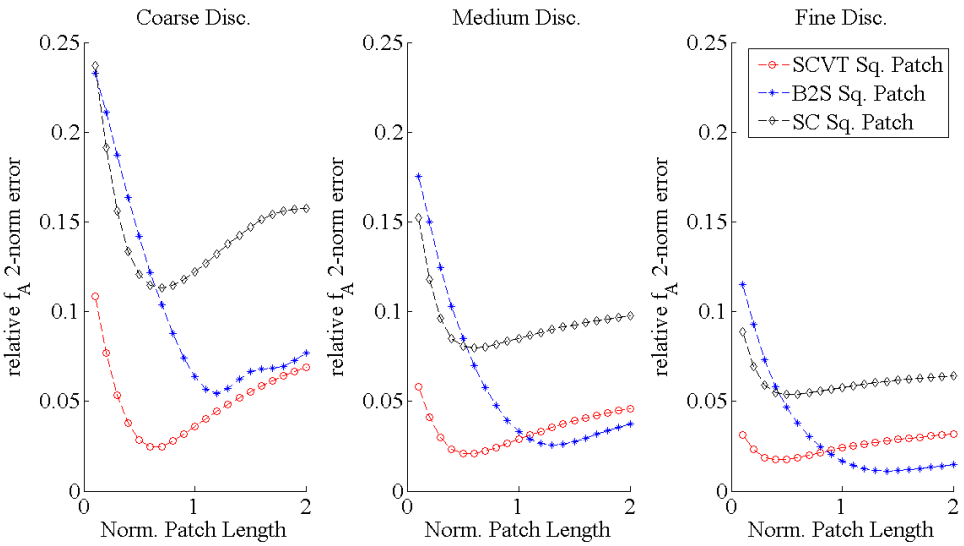

Figure 32: **The Relative f_A 2-norm Error as a Function of** $normPL$**.** Coarse discretization: $N = 600$ (SCVT and B2S) or $N = 576$ (SC). Medium discretization: $N = 2400$ (SCVT and B2S) or $N = 2401$ (SC). Fine discretization: $N = 9600$ (SCVT and B2S) or $N = 9604$ (SC). Values are calculated for $E = 0.1$ through $E = 2$ using increments of 0.1.

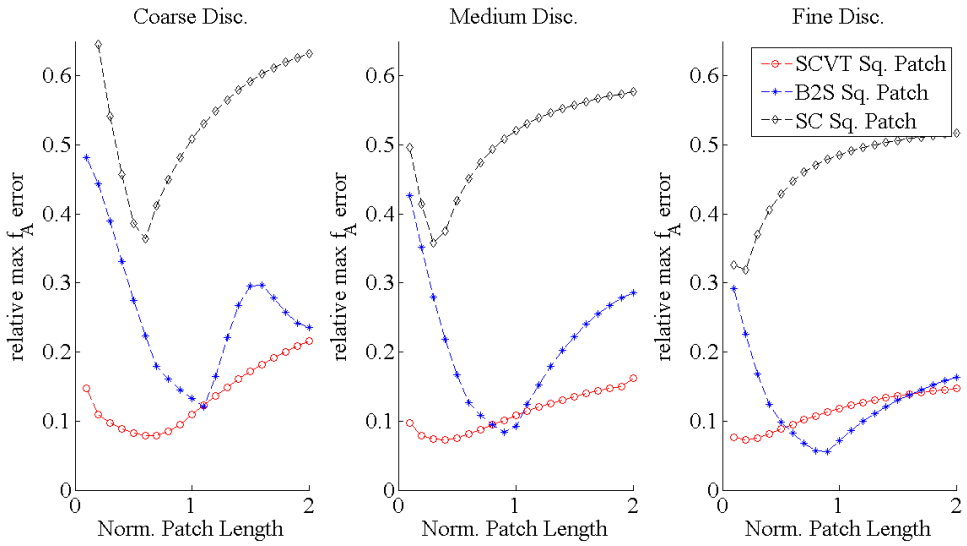

Figure 33: **The Relative f_A 2-norm Error as a Function of $normPL$.** Coarse discretization: $N = 600$ (SCVT and B2S) or $N = 576$ (SC). Medium discretization: $N = 2400$ (SCVT and B2S) or $N = 2401$ (SC). Fine discretization: $N = 9600$ (SCVT and B2S) or $N = 9604$ (SC). Values are calculated for $E = 0.1$ through $E = 2$ using increments of 0.1.

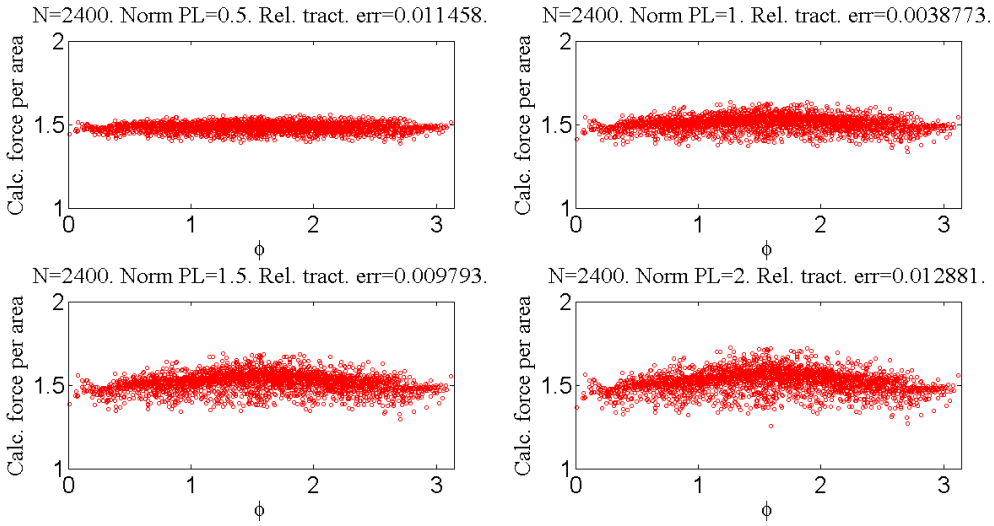

Figure 34: **MARS Force per Area results for a SCVT sphere with 2400 points, Sq. Patches, and varying normalized Patch Length.**

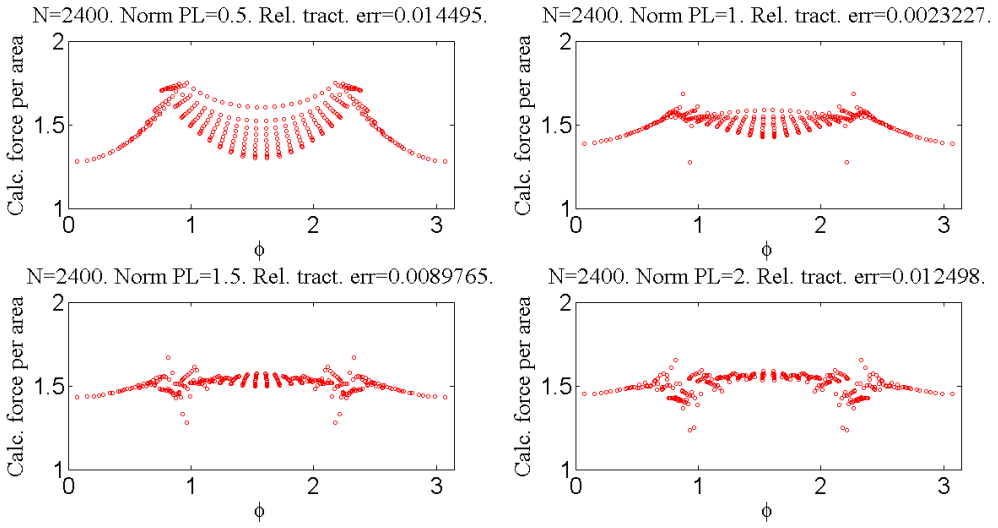

Figure 35: **MARS Force per Area results for a B2S sphere with 2400 points, Sq. Patches, and varying normalized Patch Length.**

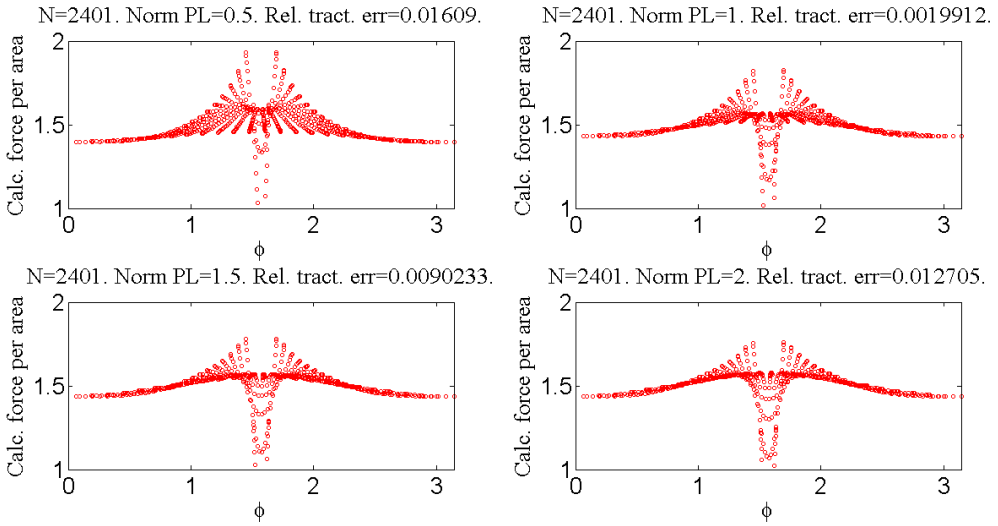

Figure 36: **MARS Force per Area results for a SC sphere with 2401 points, Sq. Patches, and varying normalized Patch Length.**

3.4 Global and Local Error Comparison

Similar to our study of the MRS, we conclude our study of the MARS by looking at any relationship between global and local errors. In chapter 2, we were not able to draw good conclusions about local behavior from the traction error, and we saw many instances where the traction error was low, but the max f_A error was high. In this chapter, we saw a repeat of that pattern.

As a first step to look for a possible relationship between local and global error in the MARS, we review the scatterplots in figures 37 and 38 which compare the local error measures (relative f_A norm-2 error and relative maximum f_A error) to the global error measurement (relative traction error). Figure 37 shows the error results of all dual-discretizations of the sphere we considered at medium refinement as $normPL$ is held constant (for Sq. Patches) and E is varied. Figure 38 shows error calculations from the cases where we varied $normPL$ instead of E. From these graphs we can see two things. The first is that the local errors are (like with the MRS) often significantly higher than the traction errors. The next thing is that, unlike the MRS, there is not a suggestion of an obvious relationship between traction error and f_A norm-2 or maximum f_A error.

We remind the reader that since we confirmed the MARS weakens the dependence of the traction error and f_A norm-2 error on E, one hopes to use fewer primary Stokeslets with the MARS in order to have a smaller matrix S in equation 6 than a similar calculation using the MRS while ensuring good error. (This is important because it reduces the time involved in solving the matrix equation 6). With this in mind, we present a summary of the results of this chapter for the medium refinement of all discretizations considered in figures 39 and 40. (Results for the coarse refinement spheres are similar.) Figure 39 shows the traction, f_A norm-2, and maximum f_A errors as function of E while figure 40 shows these errors as a function of $normPL$. Figure 39 shows that SCVT with Sq. Patches, B2S with Sq. Patches, and B2S with Fitted Patches give better results as E is varied than SC with either Sq. or Fitted Patches, which has poor maximum f_A error. Figure 40 shows that for the Sq. Patch discretizations, the SCVT performs the best overall (especially focusing on consistency of error). Overall, the best performers were SCVT with Sq. Patches and B2S with Fitted Patches.

However, since our studies showed consistently that relative maximum f_A errors occur where points are clustered (figure 30 shows that B2S with Fitted Patches is no exception to this pattern), SCVT with Sq. Patches seems to be the better choice as error is not concentrated on one part of the sphere which should lead to more consistent results. For instance if a sphere were immersed in Stokes' flow very near another object that would increase the pressure and therefore the force on one part of the sphere, the results with the SCVT with Sq. Patches could be less dependent on the orientation of the sphere unlike the B2S with Fitted Patches. Future work could confirm this hypothesis.

In figure 41 we consider the behavior of the error measurements as a function of the average spacing between primary Stokeslets, s (see equation 14). As expected, the traction error and the f_A norm-2 error decrease as the spacing between Stokeslets decreases (which means the number of primary Stokeslets increases). The maximum f_A error acts less predictably. The SC spheres have maximum f_A errors that act unpredictably as s

decreases, and the SCVT sphere has a maximum f_A error that modestly increases as s decreases. The SC spheres' unexpected behavior is likely due to the increasingly uneven discretization as s decreases which causes relatively more clustered points. The behavior of the SCVT sphere may be partly due to the approximation of P_A. Future work could repeat these error calculations with a more accurate P_A values for the SCVT. Since we are interested primarily in coarser discretizations of the sphere (larger s), this does not affect the recommendation of the SCVT discretization.

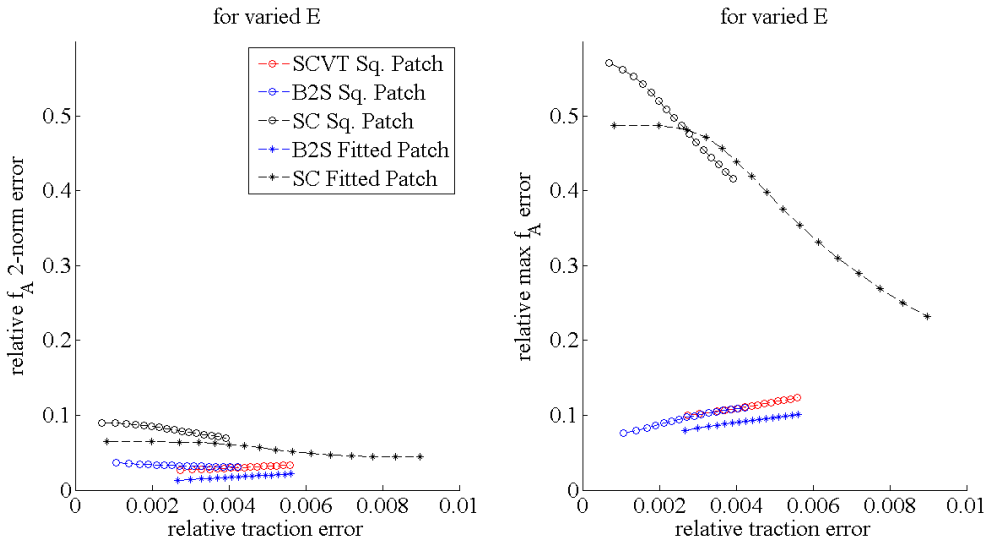

Figure 37: **MARS: A Comparison of Global and Local Errors for Varied E.** Error values calculated $N = 2400$ (SCVT and B2S) and $N = 2401$ (SC). Calculated for $E = 0.5$ to $E = 2$. $normPL = 1$ for all Sq. Patch discretizations.

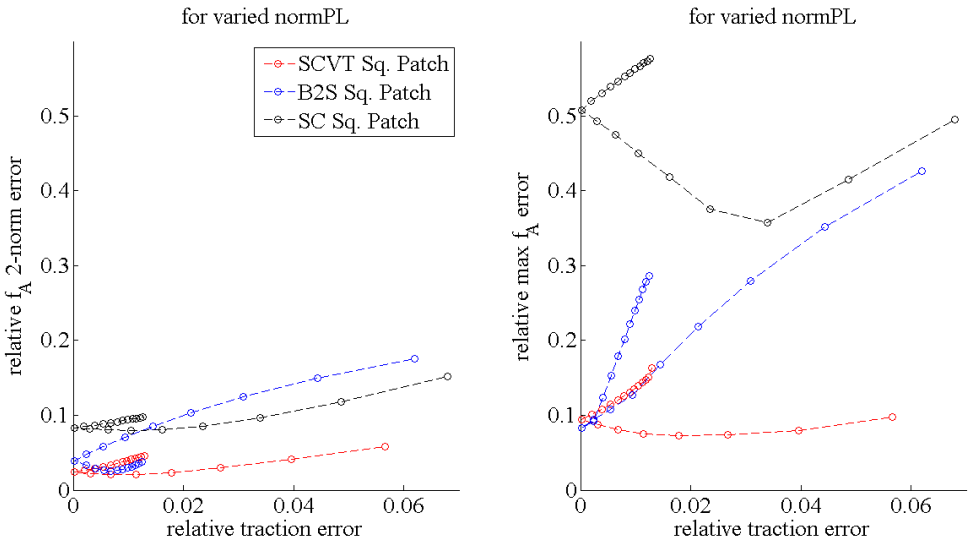

Figure 38: **MARS: A Comparison of Global and Local Errors for Varied** *normPL*. Error values calculated $N = 2400$ (SCVT and B2S) and $N = 2401$ (SC). $E = 1$ for all discretizations.

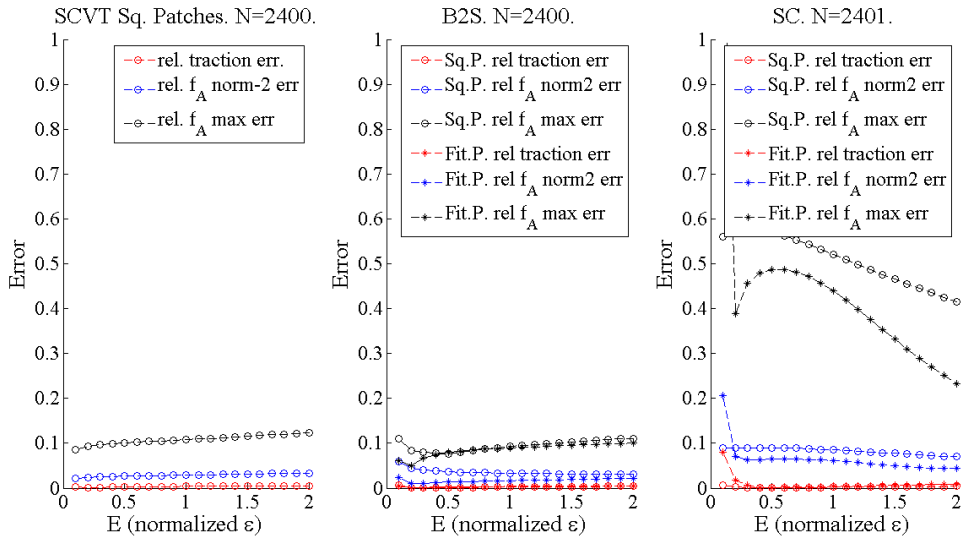

Figure 39: **MARS Error Comparison of all Medium Refinement Spheres as** E **is varied.** Values are calculated for $E = 0.1$ to $E = 2$ in increments of 0.1.

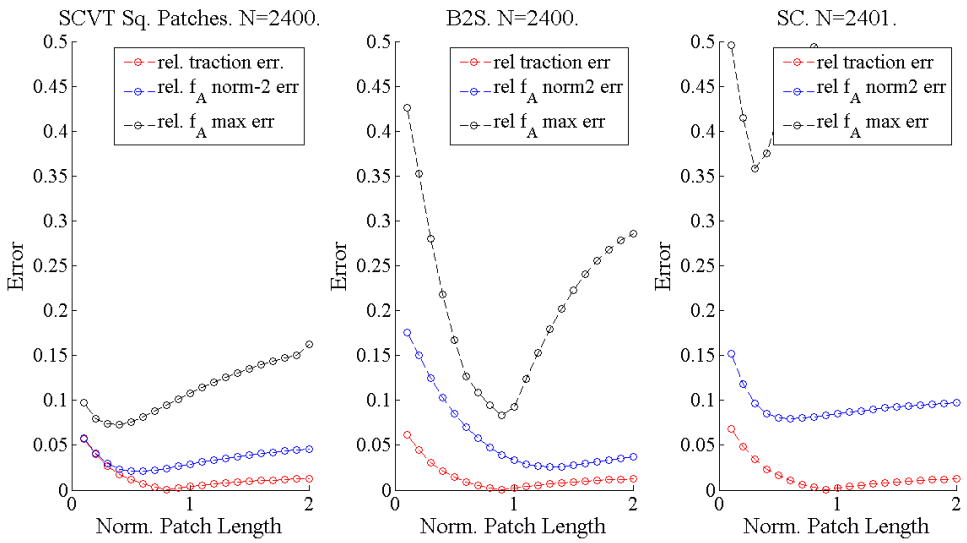

Figure 40: **MARS Error Comparison of all Medium Refinement Spheres as** $normPL$ **is varied.** Values are calculated for $normPL = 0.1$ to $normPL = 2$ in increments of 0.1.

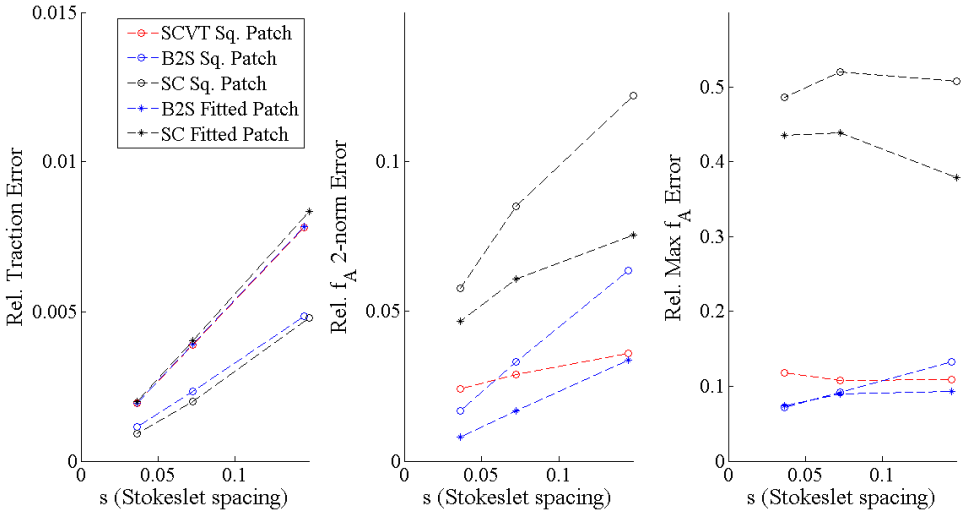

Figure 41: **MARS: Local and Global Errors as a Function of Primary Stokeslet Spacing,** s**.** As N, the number of primary Stokeslets increases, s decreases. $E = 1$ and $normPL = 1$ for all calculations shown.

4 Conclusion

Traction error has been a common measure for examining the performance of the MRS and MARS in a variety of test problems. Traction error is one common measure of performance, but local force error is also important to consider. For this reason, we study the performance of the MRS and MARS locally.

In our studies, the MRS and MARS both have trouble with accurately calculating local forces. The f_A calculation for the MRS is as (or more) sensitive to the choice of E as the traction error; the f_A calculations and maximum relative f_A error change significantly as E varies. The maximum f_A relative error is also generally much higher than the relative traction error for each E choice. This dependence of f_A on E is not fixed in the MRS by trying a simply-adaptive ϵ.

Although the MARS does not show as much sensitivity to E in the traction error, the qualitative behavior of the f_A calculations, and the f_A norm-2 error, it does show some sensitivity to E in the max f_A error when the discretization of the sphere has clustered points which create outlying points on the f_A curve. It also shows sensitivity of the traction and f_A calculations to the parameter $normPL$ which greatly affects the associated errors of both as well as the qualitative behavior of the f_A calculations. Using Fitted patches that do not use $normPL$ in their generation sidesteps this issue, but Fitted patches do not solve the issue of outlying f_A points. Furthermore, our results show making a good (intuitive) choice of $normPL$ for Sq. patches on an SCVT sphere provides the good, consistent results for the error (especially for a coarse or medium refinement of the sphere).

Both the MRS and the MARS generally are sensitive to unevenly spaced primary Stokeslets in the f_A calculations and performed especially poorly in these calculations for SC spheres. These methods should be used with caution for the backward problem and with care taken to ensure Stokeslets are fairly evenly spaced.

Our studies also clarify the behavior of the recently developed MARS method, and we confirm MARS weakens the dependence on choice of E for both the traction error and the f_A norm-2 error. Although Barrero-Gil makes heavy use of SC spheres in his study of his method [5], we show the MARS does not alleviate issues with the f_A calculations using unevenly-spaced Stokeslets shown in the MRS. The consistently small traction errors provided by the MARS can hide max f_A errors that are as high or higher than a similar calculation with the MRS. We also explicitly consider different configurations of auxiliary Stokeslets (Fitted or Sq. patches), introducing the parameter $normPL$ in the process, and show the effect of varying this parameter. We show better behavior of the MARS f_A calculations when $normPL$ is about 1, the intuitive choice.

In some situations, the MARS can use fewer primary Stokeslets than the MRS to achieve more accurate local and global results. The MARS shows the best behavior when we use equally spaced primary Stokeslets and used patches of auxiliary Stokeslets that are sized to the representative area of the primary Stokeslet. When smart choices are used for the discretization of the primary and auxiliary Stokeslets, we can get good results on the local level.

Future work might include trying patches that are roughly circular (which should model the influence of the primary Stokeslet on itself better), examining the effect using the MARS has on the forward problem (prescribing the force and finding the velocity in equation 6), and trying more optimized blobs. More investigation is merited in looking at calculated f_A in other test problems and seeing if the methods exhibit similar problems in a broader range of situations. Ideally, future work would analytically describe exactly why outlying points in the f_A calculations appear and why clustered points cause this effect. Thorough analytic analysis of the error associated with the MRS and MARS on the local level is also needed, especially as they relate to discretizations that result in unevenly spaced Stokeslets.

5 References

[1] Rafael Embid Priya Boindala Ricardo Cortez Josephine Ainley, Sandra Durkin. The method of images for regularized stokeslets. Journal of Computational Physics, 227.

[2] L. Fauci S.D. Olson, S.S. Suarez. Coupling biochemistry and hydrodynamics captures hyperactivated sperm motility in a simple flagellar model. Journal of Theoretical Biology, 283.

[3] Y. Imai T. Yamaguchi T. Ishikawa, G. Sekiya. Hydrodynamic interactions between two swimming bacteria. Biophysical Journal, 93.

[4] Ricardo Cortez. The method of regularized stokeslets. SIAM J. Sci. Comput., 23(4):1204–1225, Nov 2001.

[5] A. Barrero-Gil. Weakening accuracy dependence with the regularization parameter in the method of regularized stokeslets. Journal of Computational and Applied Mathematics, 237(1):672–679, Jan 2013.

[6] E.H. Mund M.O. Deville, P.F. Fischer. An Introduction to Fluid Dynamics. Cambridge University Press, Cambridge, UK, 1967.

[7] Ricardo Cortez, Lisa Fauci, and Alexei Medovikov. The method of regularized stokeslets in three dimensions: Analysis, validation, and application to helical swimming. Physics of Fluids, 17(3):031504:1–031504:14, Feb 2005.

[8] Elizabeth L. Bouzarth and Michael L. Minion. Modeling slender bodies with the method of regularized stokeslets. Journal of Computational Physics, 230(10):3929–3947, May 2011.